CHEMISTRY
A European Journal

A Journal of
ChemPubSoc Europe

Accepted Article

Title: Cis versus Trans: The Coordination Environment About the Tin(IV) Atom in Spirocyclic Amino Alcohol Derivatives

Authors: Britta Glowacki, Roman Pallach, Michael Lutter, Fabian Roesler, Hazem Alnasr, Cederic Thomas, Dieter Schollmeyer, and Klaus Jurkschat

To be cited as: *Chem. Eur. J.* 10.1002/chem.201803952

Link to VoR: http://dx.doi.org/10.1002/chem.201803952

Supported by
ACES

WILEY-VCH

10.1002/chem.201803952

WILEY-VCH

FULL PAPER

Cis versus *Trans*: The Coordination Environment About the Tin(IV) Atom in Spirocyclic Amino Alcohol Derivatives

Britta Glowacki[a], Roman Pallach[a], Michael Lutter[aΔ], Fabian Roesler[a], Hazem Alnasr[aΔ], Cedreric Thomas[a], Dieter Schollmeyer[bΔ], Klaus Jurkschat*[a]

Abstract: The syntheses of the novel amino alcohols $MeN(CH_2CH_2CMe_2OH)_2$ (**1**), $MeN(CMe_2CH_2OH)(CH_2CMe_2OH)$ (**2**), $MeN(CH_2CH_2CH_2OH)(CH_2CMe_2OH)$ (**3**), $MeN(CH_2CH_2CMe_2OH)(CH_2CMe_2OH)$ (**4**), $MeN(CH_2CH_2CMe_2OH)(CH_2CH_2OH)$ (**5**) and $MeN(CH_2CH_2OH)(CH_2CH_2CH_2OH)$ (**6**) as well as of the spirocyclic tin (IV) alkoxides *spiro*-[*n*-$BuN(CH_2CMe_2O)_2]_2Sn$ (**7**), *spiro*-$[MeN(CH_2CH_2CMe_2O)_2]_2Sn$ (**8**, *spiro*-[*para*-$FC_6H_4N(CH_2CMe_2O)_2]_2Sn$ (**9**), *spiro*-$[MeN(CMe_2CH_2O)(CH_2CMe_2O)]_2Sn$ (**10**), *spiro*-$[MeN(CH_2CH_2CH_2O)(CH_2CMe_2O)]_2Sn$ (**11**), *spiro*-$[MeN(CH_2CH_2CMe_2O)(CH_2CMe_2O)]_2Sn$ (**12**), *spiro*-$[MeN(CH_2CH_2CMe_2O)(CH_2CH_2O)]_2Sn$ (**13**) and *spiro*-$[MeN(CH_2CH_2O)(CH_2CH_2CH_2O)]_2Sn$ (**14**) are reported. The compounds were characterized by ^1H, ^{13}C (**1**–**14**), ^{119}Sn (**7**–**14**) NMR and IR spectroscopy, electrospray ionization mass spectrometry, and single crystal X-ray diffraction analysis (**2**, **7**–**10** and **13**, **14**). Graphset analyses were performed for compounds **2a** [(MeNH(CMe$_2$CH$_2$OH)(CH$_2$CMe$_2$OH)] [HC(O)O] and **2**. The coordination environment about the tin(IV) center of the spirocyclic compounds and their possible stereoisomers were analysed by DFT calculations (*spiro*-$[MeN(CH_2CMe_2O)_2]_2Sn$, **8**–**10** and **13**).

Introduction

Amino alcohol derivatives of tin (II) and tin (IV) have been known for a long time.[1] First investigations focused on organotin derivatives such as organostannatranes, $N(CH_2CH_2O)_3SnR$, and stannabicyclooctanes, $R'N(CH_2CH_2O)_2SnR_2$ (R, R' = alkyl, aryl). Especially the coordination mode about the tin atom and the strength of the intramolecular N→Sn coordination as a function of the identity of the substituents R and R' were studied .[2] With the growing of environmental awareness, nontoxic inorganic tin compounds[3] lacking any tin-carbon bonds are in the focus of research.[4,5–9] Amino alcoholate derivatives of tin are such inorganic compounds. They are of commercial interest as they are delayed action catalysts for polyurethane formation.[10,11,12]
In continuation of our systematic studies on amino alcohol derivatives of tin, herein we report in a combined experimental and theoretical approach on symmetrical and unsymmetrical spirocyclic tin(IV) amino alcoholates and study in detail the factors that control the coordination environment about the central tin atoms. In all spirocyclic tin compounds published so far, as for example *spiro*-$[MeN(CH_2CMe_2O)_2]_2Sn$[6], the nitrogen atoms are *cis*.

Results and Discussion

I. Novel *symmetrically* and *unsymmetrically substituted amino alcohols*

In analogy to the synthesis of similar compounds,[7,8] the symmetrical amino dialcohol 4,4'-(methylazanediyl)bis(2-methylbutane-2-ol), $MeN(CH_2CH_2CMe_2OH)_2$ (**1**) was prepared via two reaction steps (Scheme 1). The reaction of methylamine and two molar equiv methyl acrylate gave 3-methyl-[(3-methoxy-3-oxopropyl)-methylamino]propanoate (**1a**). The reaction of **1a** with methylmagnesium chloride gave compound **1** as dark brown oil. It is hydroscopic and soluble in dichloromethane and methanol but less soluble in toluene, *iso*-hexane and ethylacetate.
The compounds **1a** and **1** were characterized by ^1H, ^{13}C NMR spectroscopy (see experimental section). An IR spectrum of **1** shows a broad ν_{OH} at 3332 cm^{-1}.

[a] Dr. Britta Glowacki, M. Sc. Roman Pallach, Dr. Michael Lutter, M. Sc. Fabian Roesler, Dr. Hazem Alnasr, B. Sc. Cederic Thomas, Prof. Dr. Klaus Jurkschat.
Fakultät für Chemie und Chemische Biologie,
Technische Universität Dortmund
Otto-Hahn-Straße 6
44227 Dortmund, Germany
E-mail: klaus.jurkschat@tu-dortmund.de
[b] Dr. Dieter Schollmeyer,
Institut für Organische Chemie,
Johannes Gutenberg-Universität Mainz,
55099 Mainz, Germany
Δ Crystallography

Supporting information for this article is given via a link at the end of the document.

10.1002/chem.201803952

WILEY-VCH

FULL PAPER

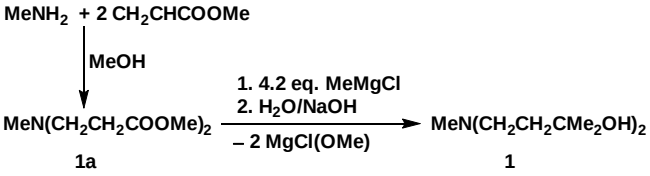

Scheme 1. Synthesis of the amino alcohol **1**.

The unsymmetrically substituted amino alcohol 2-[(2-hydroxy-2-methylpropyl)(methyl)amino]-2-methylpropane-1-ol, $MeN(CMe_2CH_2OH)(CH_2CMe_2OH)$ (**2**), was obtained according to Scheme 2 from the reaction of 2-[(2-hydroxy-2-methylpropyl)amino]-2-methylpropane-1-ol[5] with formic acid and formaldehyde solution in an Eschweiler-Clark reaction[13].

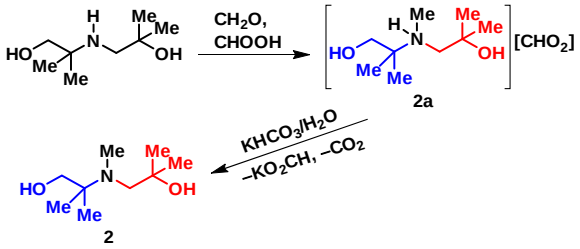

Scheme 2. Synthesis of the amino alcohol **2**.

The intermediate ammonium formate **2a** was obtained as crystalline material which shows good solubility in water. The Supporting Information contains its molecular structure (Figure S**1**) as determined by single crystal X-ray diffraction analysis, and a detailed discussion including graph set analysis.[14,15] Compound **2** shows good solubility in common organic solvents such as dichloromethane, tetrahydrofuran and hot toluene. Figure 1 shows the molecular structure of compound **2** in the solid state.

Compound **2** crystallized in the monoclinic space group $P2_1/c$ with four molecules in the unit cell. Table 1 contains selected interatomic distances and angles involving hydrogen bonds. The Proton H(17) is involved in an *intramolecular* hydrogen bond, b (O(17)–H(17)···O(11) 2.7276(15) Å) and Proton H(11) is involved in an *intermolecular* hydrogen bond, a (O(11)–H(11)···O(17)(i) 2.7298(16) Å). The interatomic <(DHA) angles in compound **2** are 171(2) and 160(2)° The hydrogen bond types a and b (Table 1) were analysed by graph set analysis.[14,15] The unitary motif N_1 contains one chain a $N_1 = C(8)$ and one hydrogen-bonded pattern b $N_1 = S(8)$. An IR spectrum of **2** shows a broad ν_{OH} at 3294 cm^{-1}.

Table 1. Selected interatomic distances [Å] and angles [deg] of the hydrogen bonds in compound **2** and unitary graph sets motifs (on diagonal) and basic binary graph set (off diagonal). Symmetry transformations used to generate equivalent atoms: (i) 1 -x+1,y+1/2,-z.+1/2.

D-H···A	d(D···A)	<(DHA)	hydrogen bonds	a	b
O(11)–H(11)···O(17)(i)	2.7300(15)	171(2)	**a**	$C(8)$,	
O(17)–H(17)···O(11)	2.7274(14)	160(2)	**b**	[a]	$S(8)$

[a]No link at binary level.

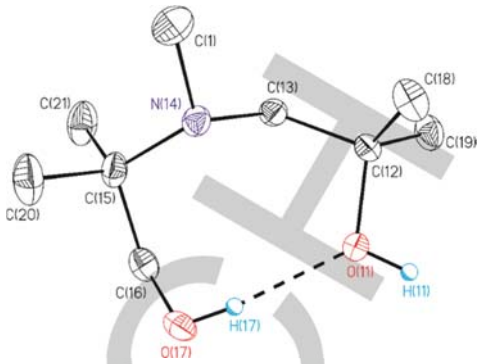

Figure 1. Molecular structure of compound **2** in the solid state (ORTEP presentation at 30% probability of the depicted atoms and atom numbering scheme). Symmetry transformations used to generate equivalent atoms: (i) 1 -x+1,y+1/2,-z.+1/2.

The reaction of 1,1-dimethyloxirane with an excess of methylamine in an ultrasonic bath gave (2-methyl-2-hydroxypropyl)(methyl)amine $MeN(H)(CH_2CMe_2OH)$ (**3a**) in good yield. The precursor compounds (methyl 3-((2-hydroxy-2-methylpropyl)(methyl)amino)propanoate) $MeN(CH_2CH_2COOMe)(CH_2CMe_2OH)$ (**3b**) and methyl 3-((2-hydroxyethyl)(methyl) amino)propanoate $MeN(CH_2CH_2COOMe)(CH_2CH_2OH)$ (**5a**) were prepared in quantitative yield by the reaction of **3a** respectively 2-(methylamino)ethanol with methyl acrylate in an ultrasonic bath. Reduction of compounds **3b** and **5a** with lithium aluminium hydride respectively methyllithium provided the amino alcohols (3-hydroxypropyl)(2-hydroxy-2-dimethylpropyl)(methyl) amine $MeN(CH_2CH_2CH_2OH)(CH_2CMe_2OH)$ (A-**3**), (2-hydroxy-2-methylbutyl)(2-hydroxy-2-methylpropyl)(methyl)amine $MeN(CH_2CH_2CMe_2OH)(CH_2CMe_2OH)$ (**4**), and (2-hydroxy-2-methylbutyl)(2-hydroxyethyl)(methyl)amine $MeN(CH_2CH_2CMe_2OH)(CH_2CH_2OH)$ (**5**) (Scheme 3).

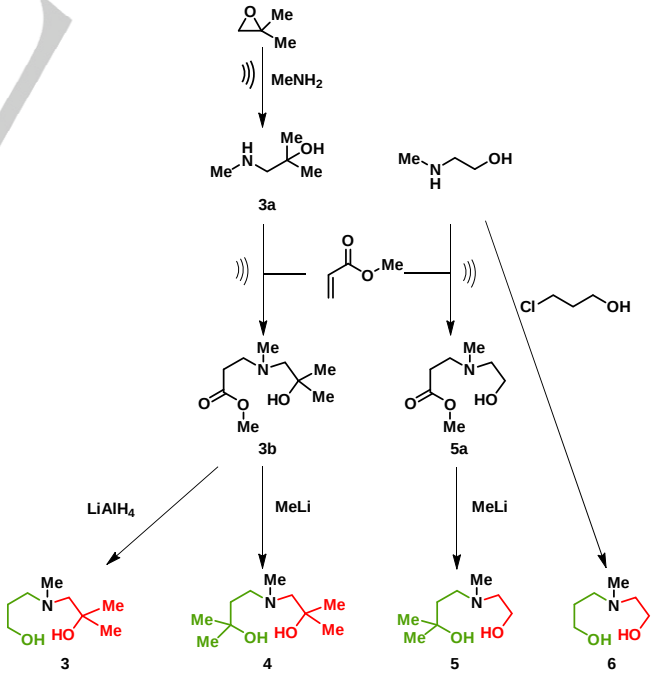

Scheme 3. Synthesis of the unsymmetrical amino alcohols **3–6** via the precursors **3a**, **3b** and **5a**.

Compounds **3–5** were obtained as yellowish oils which are soluble in common organic solvents such as toluene, tetrahydrofuran, dichloromethane, ethyl acetate or diethyl ether.

10.1002/chem.201803952

The amino alcohol (2-hydroxypropyl)(2-hydroxyethyl)(methyl)amine MeN(CH_2CH_2OH)(CH_2)$_3$OH (**6**) was prepared by the reaction of (2-hydroxyethyl)(methyl)amine with one molar equiv of 3-chloro-1-propanol in the presence of ammonium chloride (Scheme 3). Compound **6** is a colourless oil. It is soluble in common organic solvents such as those mentioned above.

II. *Spirocyclic tin(IV) compounds derived from symmetrically substituted amino alcohols*

The reaction of tin(tetra-*tert*-butoxide), Sn(O*t*-Bu)$_4$, with the symmetrically substituted amino alcohols *n*-BuN(CH_2CMe_2OH)$_2$ (**B**),[12,11] *p*-FC_6H_4N(CH_2CMe_2OH)$_2$ (**C**)[9] as well as the amino alcohol **1** gave the novel spirocyclic compounds **7**[11]-**9,** respectively (Scheme 4). These compounds are colourless crystalline materials that show good solubility in common organic solvents such as toluene, dichloromethane, and tetrahydrofuran. Single crystals suitable for X-ray diffraction analysis of **7**, **8**, and **9** were obtained from their concentrated toluene solutions. Figures 2 – 4 show the molecular structures. The figure captions contain selected interatomic distances and angles.

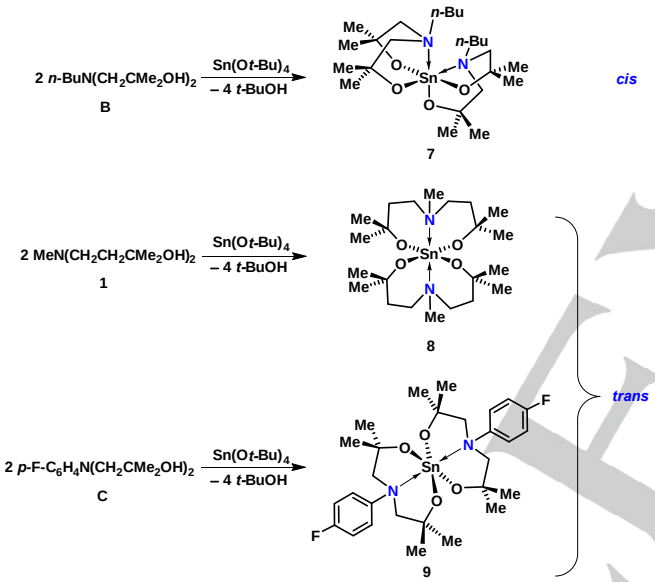

Scheme 4. Synthesis of the spirocyclic compounds **7**-**9.** In compound **7** the nitrogen atoms are *cis* and in compounds **8** and **9** the nitrogen atoms are *trans*, as found in the solid state.

Compound **7** crystallized in the orthorhombic space group $P2_12_12_1$ (Z=4). The tin atom shows a strongly distorted octahedral coordination environment with O(11)–Sn(1)–N(34) and O(37)–Sn(1)–N(14) angles of 165.63(11) and 165.55(10)°, respectively. The nitrogen atoms are *cis* (N(14)–Sn(1)–N(34) 113.80(11)°, N(64)–Sn(2)–N(84) 118.24(11)°). This is in accordance with the molecular structures of the compounds *spiro*-[MeN(CH_2CMe_2O)$_2$]$_2$Sn (**D**)[6], *spiro*-[*n*-BuN(CH_2CMe_2O)$_2$]$_2$Sn (**E**)[11] and *spiro*-[$Me_2NCH_2CH_2$N(CH_2CMe_2O)$_2$]$_2$Sn (**F**).[16]
The Sn–O distances range between 2.001(3) Å (Sn(1)–O(11)) and 2.018(3)Å (Sn(1)–O(17)). They are slightly longer as compared to the corresponding distances in compound **D** (1.982(2)-1.994(2)). The Sn(1)–N(34) (2.340(4) Å) and Sn(2)–N(64) (2.389(4) Å) distances are similar to those found for **D** (2.393(2), 2.350(2)). IR experiments under non-inert conditions reveal that compound **7** is hygroscopic and sensitive towards hydrolysis (see Supporting Information, Figure S15).

Compound **8** crystallized in the triclinic space group *P*1 (Z=1). The tin atom has a nearly ideal octahedral coordination environment. Remarkably, the nitrogen atoms are *trans*. This is the first case for such an arrangement and a significant difference to the structure of compound **D**, in which these atoms are *cis*.[6] In **8** the Sn(1)–O(11) and Sn(1)–O(17) distances are 2.0134(12) and 2.0177(12) Å, respectively. They are comparable to the Sn–O distances in **7**. In compound **8** the Sn(1)–N(14) of 2.2843(15) Å is significantly shorter than the corresponding distances in **7** (2.379(3), 2.340(3) Å) and **D**[6] (2.392(2) and 2.350(2) Å).

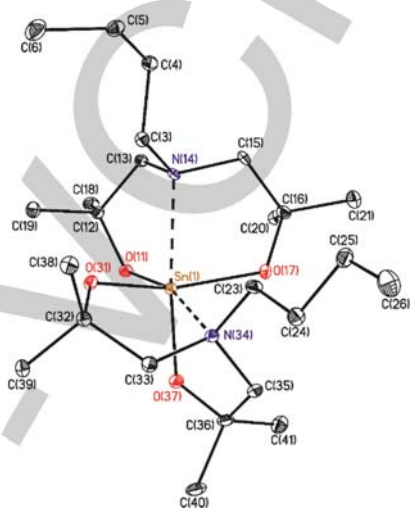

Figure 2. Molecular structure in the solid state of compound **7** (ORTEP presentation at 30% probability of the depicted atoms and atom numbering scheme). Selected interatomic distances [Å]: Sn(1)–O(11) 2.001(3), Sn(1)–O(17) 2.018(3), Sn(1)–O(31) 2.004(2), Sn(1)–O(37) 2.002(2), Sn(1)–N(14) 2.379(3), Sn(1)–N(34) 2.340(3), Sn(2)–O(61) 2.001(3), Sn(2)–O(67) 2.005(3), Sn(2)–O(81) 2.007(3), Sn(2)–O(87) 2.006(3), Sn(2)–N(64) 2.389(3), Sn(2)–N(84) 2.374(3). Selected interatomic angles [deg]: O(11)–Sn(1)–N(34) 165.63(11), O(37)–Sn(1)–N(14) 165.55(10), N(14)–Sn(1)–N(34) 113.80(11), O(61)–Sn(2)–N(84) 162.59(11), O(87)–Sn(2)–N(64) 163.49(11), N(64)–Sn(2)–N(84) 118.24(11).

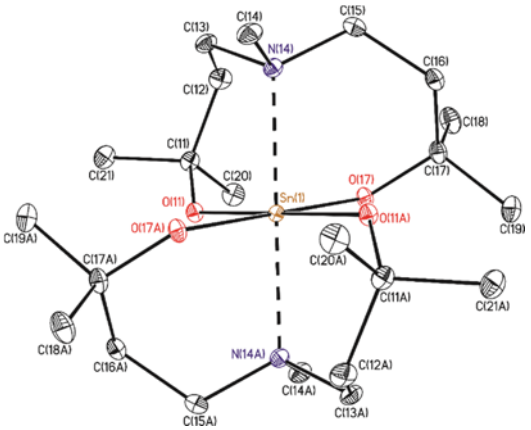

Figure 3. Molecular structure in the solid state of compound **8** (ORTEP presentation at 30% probability of the depicted atoms and atom numbering scheme). Selected interatomic distances [Å]: Sn(1)–O(11) 2.0134(12), Sn(1)–O(17) 2.0177(12), Sn(1)–N(14) 2.2843(15). Selected interatomic angles [deg]: O(11)(i)–Sn(1)–O(11) 180.00(2), O(17)–Sn(1)–O(17)(i) 180.0, N(14)(i)–Sn(1)–N(14) 180.0. Symmetry transformations used to generate equivalent atoms: (i) -x+1,-y,-z+1.

Compound **9** crystallized in the monoclinic space group $P2_1/c$ with four molecules in the unit cell (Z = 4). In this compound the nitrogen atoms are *trans*, although the amino alcoholate chains are equal to the chains in **D** and **7**. Apparently, the *p*-FC_6H_4-

10.1002/chem.201803952

substituent at the nitrogen atom in **9** is responsible for this change of structure. The Sn(1) atom has a distorted octahedral coordination environment with N(14)–Sn(1)–N(34), O(11)–Sn(1)–O(17), and O(31)–Sn(1)–O(37) angles of 165.53(16)°, 153.74(16), and 153.94(16)°, respectively. The Sn–O distances are comparable to those of the spirocyclic compounds **D**[6], **7** and **8,** and range from 1.990(4) Å (Sn(1)–O(37)) to 2.025(4) Å (Sn(1)–O(17)). The Sn(1)–N(14) and Sn(1)–N(34) distances of 2.321(4) and 2.306(4) Å, respectively, are longer than the corresponding distances in the *trans* configured *spiro*-compound **8** (2.2843(15) Å).

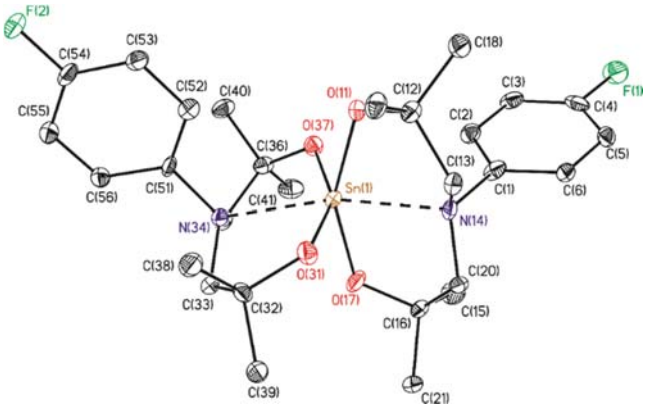

Figure 4. Molecular structure in the solid state of compound **9** (ORTEP presentation at 30% probability of the depicted atoms and atom numbering scheme). Selected interatomic distances [Å]: Sn(1)–O(11) 2.012(4), Sn(1)–O(17) 2.025(4), Sn(1)–O(31) 2.021(4), Sn(1)–O(37) 1.990(4), Sn(1)–N(14) 2.321(4), Sn(1)–N(34) 2.306(4). Selected interatomic angles [deg]: O(11)–Sn(1)–O(17) 153.74(16), O(11)-Sn(1)-O(31) 93.96(15), O(11)-Sn(1)-O(37) 87.91(15), O(17)-Sn(1)-O(31) 94.54(17), O(17)-Sn(1)-O(37) 95.14(17), O(31)–Sn(1)–O(37) 153.94(16), N(14)–Sn(1)–N(34) 165.53(16).

A ^{119}Sn{^{1}H} NMR Spectrum of a solution of **7** in C_6D_6 shows one single resonance at δ –437 ppm. For compound **8** (in C_6D_6 solution) a single resonance at δ –603 ppm was observed. A ^{119}Sn{^{1}H} NMR spectrum of **9** (in C_6D_6 solution) shows a single resonance at δ –447 ppm and a ^{19}F{^{1}H} NMR spectrum reveals a single resonance at δ –113.6 ppm.
An ESI MS spectrum (positive mode) of a solution of **7** in acetonitrile showed a mass cluster centred at *m/z* = 218.1 which is assigned to the protonated ligand [**B**+H]$^+$, and mass clusters centred at *m/z* = 551.3 [**7** +H]$^+$, 573.4 [**7**+Na]$^+$, 589.4 [**7**+K]$^+$, 614.4 [**7**+MeCN + H]$^+$ assigned to the protonated spirocyclic compound, the sodium- and potassium adducts and a protonated MeCN-adduct, respectively. The compounds **8** and **9** are not stable under ESI MS conditions.

The reaction of Sn(O*t*-Bu)$_4$ with the symmetrically substituted amino alcohol *p*-$FC_6H_4N(CH_2CMe_2OH)_2$ (**C**)[9] gave, as a by-product, a small amount of *p*-$FC_6H_4N(CH_2CMe_2O)_2Sn(Ot\text{-}Bu)_2$ (**9a**) as colourless crystalline material. It shows similar solubility in organic solvents as compound **9**. It crystallized in the monoclinic space group I_2/a, with eight molecules in the unit cell. Figure 5 shows the molecular structure of **9a**. The figure caption contains selected interatomic distances and angles.
The Sn(1) atom in compound **9a** is five-coordinated by one nitrogen and four oxygen atoms and shows a distorted trigonal bipyramidal environment (geometric goodness $\Delta\sum(\vartheta) = 50\ °$)[17] with N(1) and O(4) occupying the axial and O(1), O(2) and O(3) occupying the equatorial positions. The Sn–O distances vary between 1.937(3) (Sn(1)–O(3)) and 1.977(3) Å (Sn(1)–O(11)). The Sn(1)–N(14) distance of 2.521(3) Å is significantly longer than the corresponding distances in the spirocyclic compound **9** (Sn(1)–N(14) 2.321(4) Å, Sn(1)–N(34) 2.306(4) Å). The *trans* O(4)–Sn(1)–N(14) angle in **9a** is 171.67(11) °.

A ^{119}Sn NMR spectrum shows two resonances at δ –402 ppm (integral 23%) and δ –447 ppm (integral 77%), which are assigned to compound **9a** and the spirocyclic compound **9**, respectively.
A ^{19}F NMR spectrum of the same sample shows two signals at δ –113.6 ppm (**9**) and δ –116.4 ppm (**9a**), respectively.

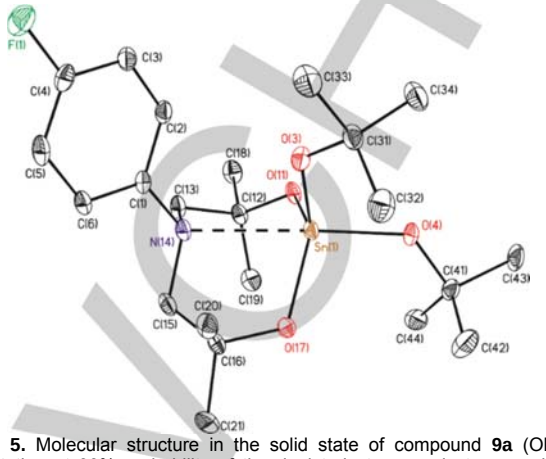

Figure 5. Molecular structure in the solid state of compound **9a** (ORTEP presentation at 30% probability of the depicted atoms and atom numbering scheme). Selected interatomic distances [Å]: Sn(1)–O(3) 1.937(3), Sn(1)–O(4) 1.967(3), Sn(1)–O(11) 1.977(3), Sn(1)–O(17) 1.970(3), Sn(1)–N(14) 2.521(3), Selected interatomic angles [deg]: O(3)–Sn(1)–O(4) 100.28(11), O(3)–Sn(1)–O(11) 111.78(12), O(3)–Sn(1)–O(17) 118.98(12), O(4)–Sn(1)–O(11) 97.73(12), O(4)–Sn(1)–O(17) 102.39(11), O(11)–Sn(1)–O(17) 120.02(12), O(3)–Sn(1)–N(14) 87.06(11), O(4)–Sn(1)–N(14) 171.67(11), O(11)–Sn(1)–N(14) 75.71(11), O(17)–Sn(1)–N(14) 77.09(11).

III. Spirocyclic tin compounds derived from *unsymmetrically substituted* amino alcohols

To figure out whether the position of the methyl substituents at the amino alcoholate chains has an influence concerning *cis* or *trans* position of the nitrogen atoms in spirocyclic tin (IV) compounds, compound **10** was synthesized by the reaction of Sn(O*t*-Bu)$_4$ with the unsymmetrical amino alcohol **2** (Scheme 5). It was obtained as a colourless crystalline material.

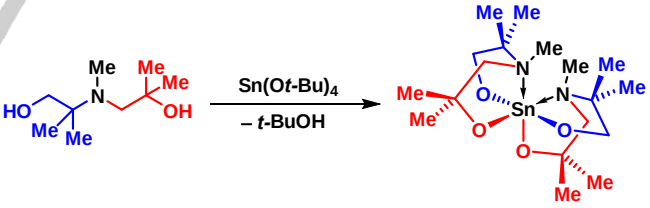

2 **10**

Scheme 5. Synthesis of the spirocyclic compound **10**.

Single crystals of **10** suitable for X-ray diffraction analysis were obtained from its toluene solution. Figure 6 shows the molecular structure of **10**. The figure caption contains selected interatomic distances and angles. Compound **10** crystallized in the orthorhombic space group *Pbca* with eight molecules in the unit cell. The nitrogen atoms are stereogenic centres in which the coordinating lone electron pair is assigned the lowest priority. As a consequence, there are four pairs of enantiomers with *R*,*R* and *S*,*S* configuration.
The Sn(1) atom shows a distorted octahedral environment with O(11)–Sn(11)–N(36), O(31)–Sn(11)–N(16), and O(22)–Sn(11)–O(42) *trans* angles of 161.81(8), 159.10(8)°, and 136.38(9)°, respectively. The N(16) and N(36) atoms are *cis* with an N(16)–Sn(1)–N(36) angle of 121.72(8)°. This angle is slightly bigger than those in compounds **D** (119.41(9)) and **7** (118.24(13)). The Sn–O distances are very similar to compound **D** and fall in the narrow

10.1002/chem.201803952

range between 1.9903(19) Å (Sn(11)–O(31)) and 2.002(2) Å (Sn(11)–O(22)). However, the Sn(11)–N(16) (2.543(2) Å) and Sn(11)–N(36) (2.461(2) Å) distances in **10** are significantly longer as compared to those measured for **D** (2.392(2) Å, 2.350(2) Å).

A ^{119}Sn NMR spectrum (in C_6D_6) of the crude reaction mixture shows a total of five resonances at δ –398 ppm (integral 36%), –437 ppm (integral 23%), –443 ppm (integral 35%) and –460 ppm (integral 3%), –500 ppm (integral 3%). The resonance at δ –398 ppm is assigned to the intermediate MeN(CH_2CMe_2O)(CMe_2CH_2O)Sn(O*t*-Bu)$_2$. Because of the two different amino alcoholate chains, for compound **10** three *cis* (**10a** – **10c**) and two *trans* (**10d** and **10e**) isomers are possible (see Figure 7).

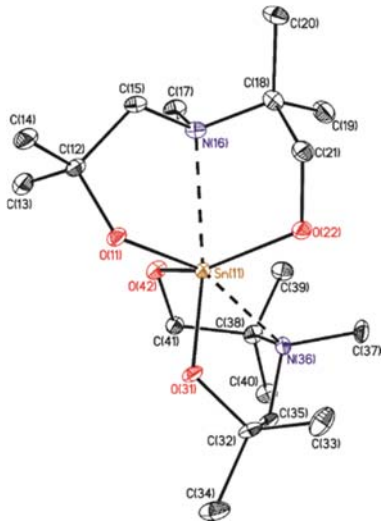

Figure 6. Molecular structure in the solid state of compound **10** (ORTEP presentation at 30% probability of the depicted atoms and atom numbering scheme). Selected interatomic distances [Å]: Sn(11)–O(11) 1.9954(19), Sn(11)–O(22) 2.002(2), Sn(11)–O(31) 1.9903(19), Sn(11)–O(42) 1.998(2), Sn(11)–N(16) 2.543(2), Sn(11)–N(36) 2.461(2). Selected interatomic angles [deg]: O(22)–Sn(11)–O(42) 136.38(9), O(11)–Sn(11)–N(36) 161.81(8), O(31)–Sn(11)–N(16) 159.10(8), N(36)–Sn(11)–N(16) 121.72(8).

A ^{119}Sn NMR spectrum of a solution of the crystalline material in C_6D_6 reveals two resonances at δ –437 ppm (integral 40%) and –443 ppm (integral 60%), respectively. A powder diffraction analysis of the crystalline material was performed. A comparison with the parameters obtained from the single crystal X-ray analysis via Pawley fit[18] showed the homogeneity of the bulk material and its identity with the structure established by single crystal X-ray diffraction analysis. Evidently, only one isomer crystallized. ^{119}Sn NMR spectra of the crystalline material dissolved in tetrachlorethane-d_2, acetone-d_6, acetonitrile-d_3, dichloromethane-d_2 and chloroform-d_1, respectively, were collected (see Sporting Information Figure S21). The spectra in acetonitrile-d_3 (δ –438 ppm ($\nu_{1/2}$ = 134 Hz, integral 45%), δ –443 ppm (integral 55%)) and dichloromethane-d_2 (δ –438 ppm ($\nu_{1/2}$ = 150 Hz, integral 38%), δ –443 ppm (integral 62%)), respectively, show each two resonances. Only one signal (δ –445 ppm) was observed in both acetone-d_6 and chloroform-d_1 whereas the spectrum in tetrachlorethane-d_2 shows a total of three resonances (δ –446 ppm (integral 70%), δ –443 ppm (integral 18%), δ –454 ppm (integral 12%)). Apparently, in solution several isomers exist. The population of these isomers depend on the identity of the solvent. The interconversion of the isomers into each other is slow on the ^{119}Sn NMR time scale. No detailed studies concerning the mechanism of the isomerization process were performed. Possible mechanisms include (i) a combined Sn–N dissociation followed by a Berry pseudorotation[19] and Sn–N re-coordination, or (ii) protonation/de-protonation of a tin-bound oxygen atom accompanied with tin-oxygen bond cleavage/re-formation (traces of protons are rather difficult to exclude experimentally), or (iii) a Ray-Dutt-twist- or Bailar-twist-mechanism.[20]

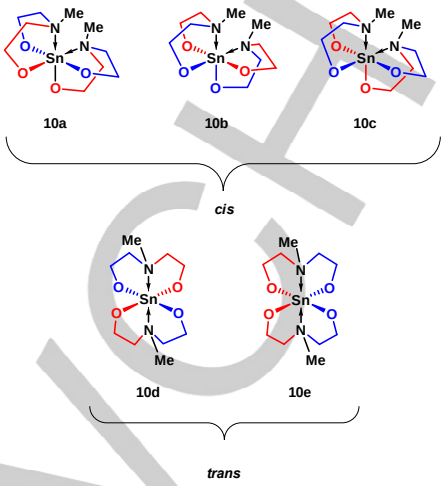

Figure 7. Three possible cis isomers **10a, 10b, 10c** (top) and two possible *trans* isomers **10d and 10e** (bottom). The methyl substituents are omitted for clarity. The red amino alcoholate chain symbolizes NCH_2CMe_2O and the blue one $NCMe_2CH_2O$.

An ESI MS spectrum (positive mode) of **10** shows a major mass cluster centred at m/z = 467.2 which is assigned to the protonated species of spirocyclic compound [**10** + H]$^+$.

A further alternative of generating unsymmetrical spirocyclic tin(IV) compounds involves amino dialcohols containing two side chains of different length. Accordingly, the reaction of Sn(O*t*-Bu)$_4$ with the unsymmetrically substituted amino dialcohols **3** – **6** gave the novel *spiro*-type compounds **11** – **14** (Scheme 6).

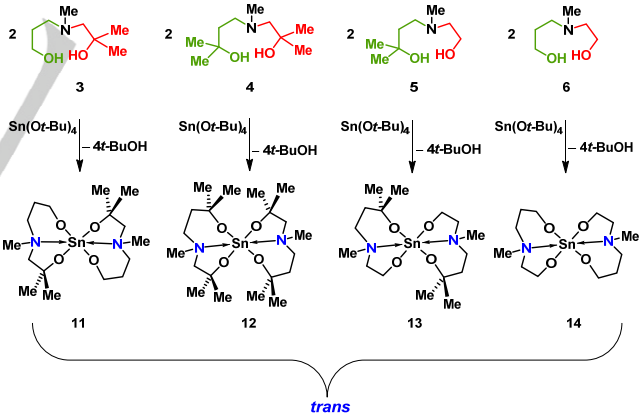

Scheme 6. Synthesis of the *spiro*-cyclic compounds **11**–**14**.

Compounds **13** and **14** are colourless crystalline materials, whereas compounds **11** and **12** were isolated as waxy-type residues.

Compounds **11** – **14** show good solubility in common organic solvents such as toluene, tetrahydrofuran or dichloromethane. The Figures 8 and 9 show the molecular structures of compounds **13** and **14**, respectively, as determined by single-crystal X-ray diffraction analysis. The Figure captions contain selected interatomic distances and angles. The Supporting Information (Figure S39) contains the molecular structure of the toluene solvate **13**·C_7H_8. In both the molecular structures of the spirocyclic compounds **13** and **14** the nitrogen atoms are *trans*.

10.1002/chem.201803952

Compound **13** crystallized in the orthorhombic space group *Pbca* with four crystallographic independent molecules in the asymmetric unit of the unit cell and **13**·C_7H_8 crystallized in the triclinic space group *P*1 with Z=1. In both **13** and **13**·C_7H_8 the Sn(1) atoms have an all-*trans* octahedral coordination sphere. In both structures, the Sn–O distances are slightly longer (Sn(1)–O(11) 2.0337(11), **13**; Sn(1)–O(11) 2.0249(16), **13**·C_7H_8) when the shorter amino alcoholate chain -CH_2CH_2O is involved than in the case when the longer amino alcoholate chain -$CH_2CH_2CMe_2O$ is involved (Sn(1)–O(18) 2.0206(12) Å, and Sn(1)–O(17) 2.0216(15) Å, respectively). The Sn(1)–N(14) distance in **13** is longer (2.2543(14) Å) than in **13**·C_7H_8 (2.236(2) Å). A similarity of both structures is that in each molecule one nitrogen atom shows a (*R*) and the other one a (*S*) configuration.

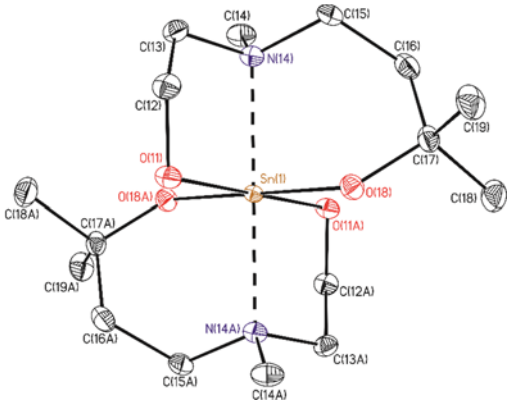

Figure 8. Molecular structure in the solid state of compound **13** (ORTEP presentation at 30% probability of the depicted atoms and atom numbering scheme). Selected interatomic distances [Å]: Sn(1)–O(11) 2.0337(11), Sn(1)–O(18) 2.0206(12), Sn(1)–N(14) 2.2543(14). Selected interatomic angles [deg]: O(11)–Sn(1)–O(11)(i) 180.00(7), O(18)(i)–Sn(1)–O(18) 180.0, N(14)(i)–Sn(1)–N(14) 180.0. Symmetry transformations used to generate equivalent atoms: (i) -x+1,-y,-z+1.

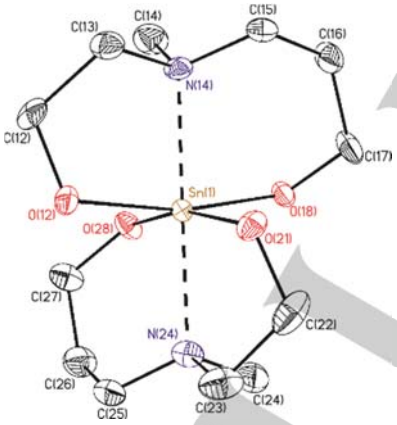

Figure 9. Molecular structure in the solid state of compound **14** (ORTEP presentation at 30% probability of the depicted atoms and atom numbering scheme). Selected interatomic distances [Å]: Sn(1)-O(12) 2.030(4), Sn(1)–O(18) 2.014(4), Sn(1)–O(21) 2.029(4), Sn(1)–O(28) 2.011(4), Sn(1)–N(14) 2.249(5), Sn(1)–N(24) 2.261(5), Selected interatomic angles [deg]: O(12)–Sn(1)–O(18), 167.75(17), O(21)–Sn(1)–O(28) 166.38(18), N(14)–Sn(1)–N(24) 173.39(19).

Compound **14** crystallized in orthorhombic space group *Pbca* with 8 molecules per unit cell. The Sn(1) atom has a slightly distorted octahedral coordination sphere with O(12)–Sn(1)–O(18), O(21)–Sn(1)–O(28), and N(14)–Sn(1)–N(24) angles of 167.75(17)°, 166.38(18)°, and 173.39(19)°, respectively. The Sn(1)–N(14) and Sn(1)–N(24) distances of 2.249(5) and 2.261(5) Å, respectively, are comparable to those of **13** (2.2543(14) Å) and **13**·C_7H_8 (2.236(2) Å). In the molecular structure of **14**, the nitrogen atoms in one molecule are both (*R*) or both (*S*) configured, giving again four pairs of enantiomers in the unit cell.

In **13** the oxygen atoms of a given amino alcoholate chain are *cis* (Figure 10, type I). Interestingly, **14** is the first example wherein the corresponding oxygen atoms of a given amino dialcoholate are *trans* (compare Figure 10, type II). This phenomenon was already reported by Zaitsev et al[21] for related spirocyclic titan(IV) compounds.

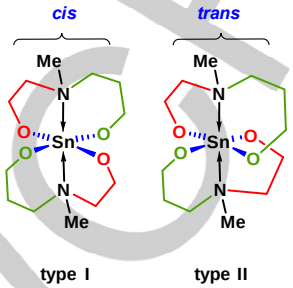

Figure 10. Coordination sphere of the tin atom in spirocyclic *trans* isomers. Type I: the oxygen atoms of a given amino alcoholate chain are *cis*. Type II: the oxygen atoms of a given amino alcoholate chain are *trans*.

The ^{119}Sn NMR spectra of compounds **11**–**14** show respectively two or three signals (**11**: δ –512 ppm (integral 48%), –512 ppm (integral 46%) and –515 ppm (integral 6%); **12**: δ –529 ppm (integral 66%), –532 ppm (integral 13%) and –555 ppm (integral 21%); **13**: δ –513 ppm (integral 25%), –536 ppm (integral 65%, $\nu_{1/2}$ = 150 Hz); **14**: δ –516 ppm (integral 47%), –524 ppm (integral 30%) and –525 ppm (integral 23%)) which are assigned with caution to different stereoisomers of these compounds.
Comparing the ^{119}Sn NMR spectra of the spirocyclic compounds **D** and **7**-**14** (Figures 11, 12; see experimental section) reveals a clear correlation between the ^{119}Sn chemical shifts and the amino alcoholate chain length and ring size associated with the latter.

The compounds **D**, **7**, **9** and **10**, exclusively containing five-membered rings, show resonances between δ –437 (**7**) and –447 ppm (**9**). The compounds **11**–**14**) consisting of five- and six-membered rings high field shifts between δ –512 (**11**) and –556 ppm (**13**) are observed. A ^{119}Sn NMR spectrum of compound **8** exclusively consisting of six-membered rings shows a high field shifted resonance at δ –603 ppm. A correlation between ring size and ^{119}Sn NMR chemical shift has been reported for stannacycloalkanes as well as for diorganodithiostannolanes.[22]

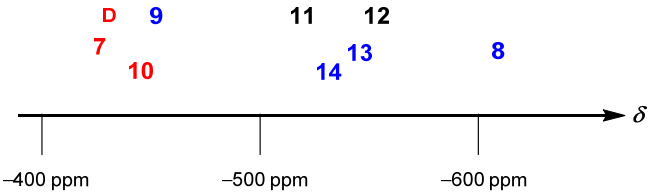

Figure 12. Trends for the ^{119}Sn NMR chemical shifts for compounds **D** and **7**–**14**. Red colour: compounds crystallized as cis isomers; blue colour: compounds crystallized as *trans* isomers; black colour: no solid-state structure was obtained so far.

Notably, the Sn–N distances in the spirocyclic compounds reported herein vary between 2.249(5) (**14**) and 2.543(2) (**10**) (Figure 11), although given the SnO_4 substituent pattern the Lewis acidity of the Sn(IV) atoms should be the same for all compounds. The Sn–N distances are longer in the compounds **D**, **7**, **9** consisting of five-membered rings only than in the spirocyclic compounds consisting of both five- and six-membered rings (**13, 14**) or only-six membered rings (**8**). This phenomenon is

10.1002/chem.201803952

explained by the different angles in five- and six-membered rings.

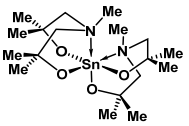

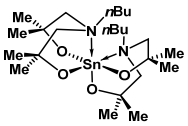

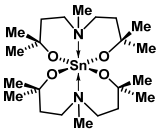

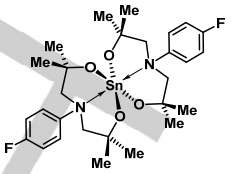

	D	**7**	**8**	**9**
^{119}Sn{^{1}H} NMR [δ]	–442	–437	–603	–447
Sn–O [Å]	1.982(2) – 1.996(2)	2.001(3) – 2.018(3)	2.0134(12), 2.0177(12)	1.990(4) – 2.025(4)
Sn–N [Å]	2.392(2) – 2.350(2)	2.340(3) – 2.389(3)	2.2843(15)	2.306(4), 2.321(4)
N–Sn–N [°]	119.41(9)	113.80(11), 118.24(11)	180.00	165.53(16)

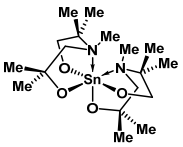

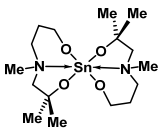

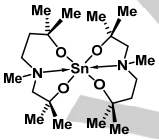

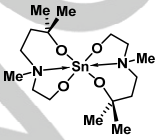

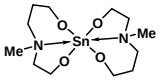

	10	**11**	**12**	**13**	**14**
^{119}Sn{^{1}H} NMR [δ]	–437 (40%), –443 (60%)	–512 (48%), –512 (46%), –515 (6%)	–529 (66%), –532 (13%), –555 (21%)	–513 (35%), –556 (65%)	–516 (47%), –524 (30%), –525 (23%)
Sn–O [Å]	1.9903(19) – 2.002(2)	-	-	2.0337(11), 2.0206(12)	2.011(4) – 2.030(4)
Sn–N [Å]	2.461(2), 2.543(2)	-	-	2.2543(14)	2.249(5), 2.261(5)
N–Sn–N [°]	121.72(8)	-	-	180.00	173.39(19)

Figure 11. Selected experimental data of the spirocyclic tin compounds **D**[6], **7-14**.

IV. DFT-Calculations:

To investigate the coordination environment of the tin atoms in selected spirocyclic compounds and to compare *cis* and *trans* isomers as well as the corresponding stereoisomers, DFT calculations with the program Gaussian*09*[23] were performed. The hybrid functional B3LYP[24–26], the pure functional BP86[24,27], and the dispersive functional wB97xD[28] with the basis set def2-TZVP[29,30], which includes the effective core potential on tin, were used for geometry optimization and frequency analysis.

As shown above, the identity/length of the amino alcoholate chain controls the formation of *cis* (**D** and **7**) or *trans* isomers (**8, 13, 14**) in the solid state. For the geometry optimizations, the molecular structures of **D** (*cis*) and **8** (*trans*) were used. Also, the geometries of the corresponding *trans*– (for **D**) and *cis*– (for **8**) isomers were calculated. Tables S2 and S3 in the Supporting Information contain selected interatomic distances and angles. For both structures **D** (*cis*) and **8** (*trans*) the calculated interatomic distances fit best to the corresponding molecular structure in the solid state when using the dispersive wB97xD functional.

The relative zero point-corrected energies are visualized in Figure 13. Therein, the relative energies of the *only calculated* structures are compared to the geometry optimized isomer which was found in the solid state. The calculated relative energy levels of **D** (*trans*) compared to **D** (*cis*) are: 39 kJ/mol (with B3LYP), 34 kJ/mol (with BP86), and 36 kJ/mol (with wB97xD), indicating unambiguously for **D** the *trans*–isomer to be significantly higher in energy than the *cis*–isomer. The *trans*–isomer is not preferred. For compound **8** the case is different as the energy differences are smaller. The relative energy levels of **8** (*cis*) compared to **8** (*trans*) are: 2 kJ/mol (with B3LYP), 9 kJ/mol (with BP86), and 15 kJ/mol (with wB97xD).

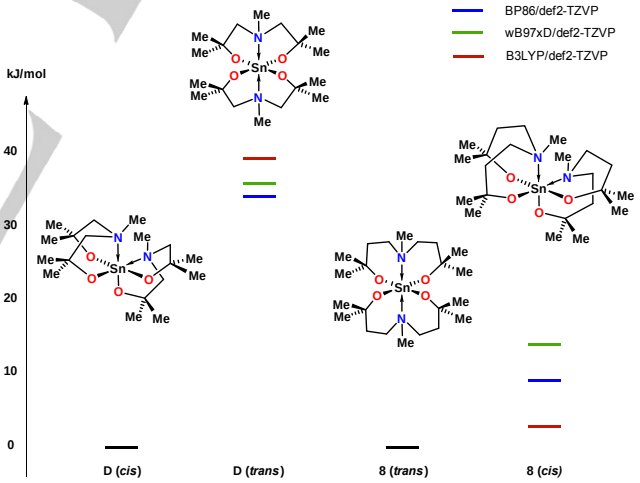

Figure 13. Visualized relative zero point-corrected energies of the calculated structures of the *cis* and the *trans* isomers of compounds **D** and **8**. The relative energy levels of **D** (*trans*) compared to **D** (*cis*) are: 39 kJ/mol (with B3LYP), 34 kJ/mol (with BP86), and 36 kJ/mol (with wB97xD) and the relative energy levels of **8** (*cis*) compared to **9** (*trans*) are: 2 kJ/mol (with B3LYP), 9 kJ/mol (with BP86), and 15kJ/mol (with wB97xD).

Analogously, the energy differences of the *cis* and the corresponding *trans* isomers of compound **9** were calculated. Furthermore, the geometry of a hypothetic pentacoordinated species ($\mathbf{9}_{penta}$) was calculated in order to evaluate whether a N→Sn dissociation might be a meaningful/reasonable step in an isomerization process. Therein, one nitrogen atom is coordinating the tin atom and the second nitrogen atom is not coordinating. The geometry optimization of **9** (*trans*) based on the geometry as found in solid state. Table S4 in the Supporting Information contains selected interatomic distances and angles, and Figure 14 visualizes the resulting zero point-corrected energies.

10.1002/chem.201803952

The N(14)–Sn(1)–N(34) angle in the molecular structure of **9** is 165.65(16)°. The DFT calculations describe this angle very well. It varies between 164.82 and 168.26° (Supporting Information, Table S4). For the hypothetic *cis* isomer the calculated N–Sn–N angle ranges between 128.75 and 131.56°. This angle is bigger than that measured for **D** (119.41(9)°) and calculated for **8** (108.66° (B3LYP)).

The energy differences between **9**(*cis*) and **9**(*trans*) are very small (1 kJ/mol (with B3LYP), 3 kJ/mol (with BP86), and 6 kJ/mol (with wB97xD)), indicating that both isomers have rather similar probability to be formed in the reaction, but only the *trans* isomer was found in the solid state. The situation is similar to that discussed for **8**, but even more pronounced. In accordance with the fact that so far in the solid state no pentacoordinated species was found for such spirocyclic compounds, the energy differences between the hypothetic pentacoordinated species and the *trans* isomer are significantly higher (38 kJ/mol (with B3LYP), 40 kJ/mol (with BP86), and 67 kJ/mol (with wB97xD)).

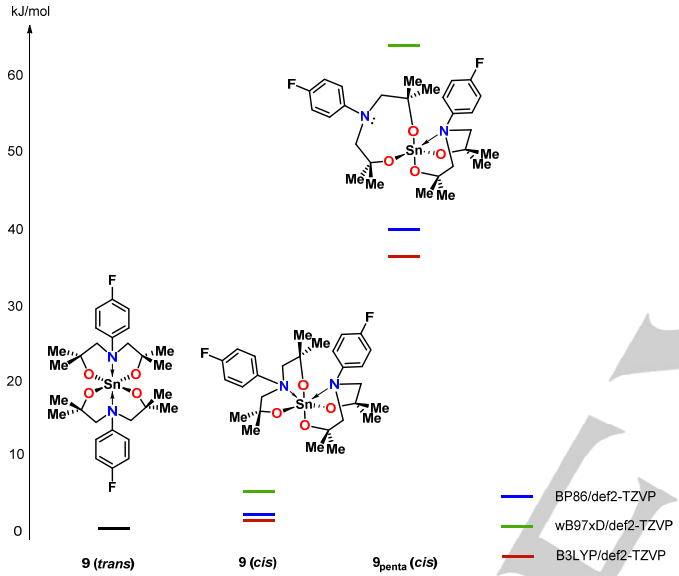

Figure 14. Visualized relative zero point-corrected energies for the calculated *cis* and *trans* isomers of compound **9** and for a pentacoordinated species $\mathbf{9}_{penta}$(*cis*). The relative energy levels of **9**(*cis*) compared to **9**(*trans*) are not significant: 1 kJ/mol (with B3LYP), 3 kJ/mol (with BP86), and 6 kJ/mol (with wB97xD). The relative energy levels of $\mathbf{9}_{penta}$(*cis*) compared to **9**(*trans*) are: 38 kJ/mol (with B3LYP), 40 kJ/mol (with BP86), and 67 kJ/mol (with wB97xD).

To estimate the relative energy differences between the five possible isomers of **10** mentioned above (Figure 15), DFT calculations were performed. Tables S5 and S6 in the Supporting Information contain selected interatomic distances and angles. The calculations for **10a** are based on the molecular structure of **10** as found in solid state. The Sn–O distances are best described with wB97xD/def2-TZVP. The calculated interatomic *trans* angles are in good agreement with the molecular structure obtained experimentally. The calculated *trans* angles for the *trans* isomers **10d** an **10e** vary between 164.23° and 176.11°. In both *trans* isomers the tin atom has a distorted octahedral coordination environment which is similar to the situation in **D** and **7** but different to **8**.

Generally, the isomer **10a**, which is identical to the molecular structure of **10**, has the lowest energy. Table S7 in the Supporting Information contains the relative energies of the other isomers **10b–10e** compared to **10a.** Figure 15 visualizes the relative zero point-corrected energies. The energy levels of the *cis* isomers **10b** and **10c** are very similar (31 kJ/mol for **10b** and 28 kJ/mol for **10c**). Both *trans* isomers **10d** (45 kJ/mol (B3LYP), 38 kJ/mol (BP86) 35 kJ/mol (wB97xD)) and **10e** (50 kJ/mol (B3LYP), 59 kJ/mol (BP86 and wB97xD)) are higher in energy. The highest relative energy of **10e** is likely the result of steric repulsion of the methyl substituents of the NCH_2CMe_2O chain.

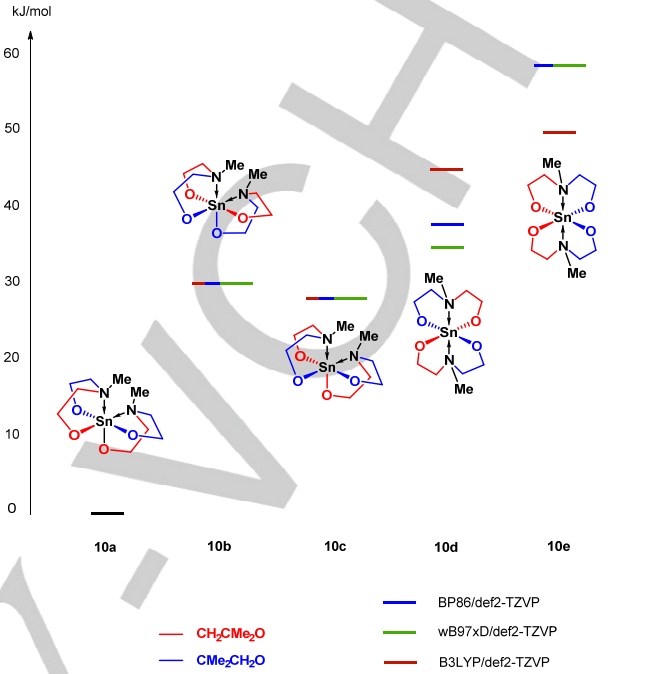

Figure 15. Visualized relative zero point corrected energies of the calculated structures of the *cis* and the *trans* isomers of compound **10**. The methyl substituents at the side chains are omitted for clarity. The red-coloured chain refers to CH_2CMe_2O and the blue-coloured one to CMe_2CH_2O.

The position of the methyl groups in the amino alcoholate chains is not decisive for a *cis* or a *trans* position of the nitrogen atoms in such spirocyclic compounds, because in **10** the *cis* position is preferred, like it is in **D**.

For each of the spirocyclic compounds **13** and **14**, three *trans* isomers **a**–**c** and three *cis* isomers **d**–**f** are possible. Exemplarily, DFT calculations were performed for compound **13**. The calculations for the **13a** (type I, Figure 10) and the **13b** (type II, Figure 10) isomers are based on the corresponding molecular structures in the solid state. The molecular structure of **14**, after having artificially added four methyl moieties, was used as the basis for the simulation of **13b**. In the *trans* isomer **13c** the $-CH_2CH_2CMe_2O$ chains are *cis*. The *cis* isomers are comparable to the calculated isomers **10a–10c**. For the calculations including toluene as solvent the IEFPCM solvent model was used.[31–35] The Tables S8 and S9 in the Supporting Information contain the calculated intramolecular distances and angles and the relative zero point-corrected energies. Figure 16 visualizes the latter.

All energies are given in relation to **13a**. The energy of **13b** is slightly lower with B3LYP (–2, –4 (toluene) kJ/mol), and with BP86 (2, 0 (toluene) kJ/mol) but similar to **13a** when wB97xD (5, 3 (toluene) kJ/mol) is used **13b** is slightly higher in energy. Generally, the *trans* isomers **13a** and **13b** have the lowest energy level, which is consistent with the corresponding molecular structures as found in the solid state. Because of steric interactions of the CH_3-substituents in **13c**, this *trans* isomer is higher in energy (B3LYP: 13, 16 (toluene) kJ/mol; BP86: 19, 19 (toluene) kJ/mol; wB97xD: 15, 15 (toluene) kJ/mol). Generally, all *cis* isomers **13d-f** are higher in energy than the *trans* isomers **13a** and **13b**. The isomer **13d** is the lowest in energy of the *cis* isomers (B3LYP: 9, 10 (with toluene) kJ/mol; BP86: 14, 15 (with toluene) kJ/mol; wB97xD: 17, 17 (with toluene) kJ/mol B3LYP). The next

10.1002/chem.201803952

in energy is **13f** (B3LYP: 16, 16 (with toluene) kJ/mol; BP86: 20, 21 (with toluene) kJ/mol; wB97xD: 31, 28 (with toluene) kJ/mol B3LYP) and **13e** is the highest in energy (B3LYP: 30, 30 (with toluene) kJ/mol; BP86: 36, 34 (with toluene) kJ/mol; wB97xD: 45, 42 (with toluene) kJ/mol B3LYP).

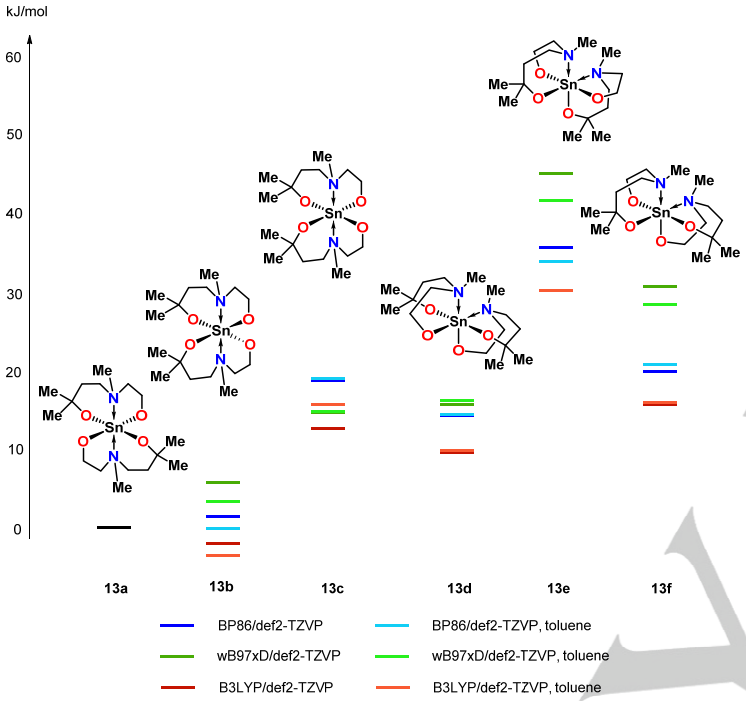

Figure 16. Visualized relative zero point-corrected energies of compound **13** for the *cis* and the *trans* isomers **13a**–**13f** in the gas phase, and with the solvent model IEF/PCM (toluene).

Conclusion

Herein, we report in a combined experimental and theoretical study how the coordination environment of spirocyclic tin (IV) compounds can be influenced.

General observations for *symmetrically substituted spirocyclic compounds* are: (i) With alkyl substituents such as methyl or *n*-butyl at the nitrogen atoms the *cis* isomer is preferred in the solid state. (ii) A lengthening of both alcoholate side chains by one CH_2 moiety results in the nitrogen atoms being *trans*. The DFT calculations show only rather small energy differences between the isomers. (iii) The replacement of the aliphatic substituent at the nitrogen atoms by an aromatic one such as *p*-FC_6H_4 provokes the crystallization of the *trans* isomer in the solid state as well. (iv) A pentacoordinated species such as **9** is not preferred.

The observations for *unsymmetrically substituted spirocyclic compounds* are: (i) If both amino alcoholate side chains are short, the position of the methyl substituents is not decisive for a *cis* or a *trans* position of the nitrogen atoms. (ii) The lengthening of only one alcoholate side chain by a CH_2 moiety causes crystallization of the *trans* isomer in solid state. (iii) For the *trans* isomers, type I and type II coordination modes of the amino alcoholates are observed in solid state and approved by DFT calculations. Given the high economic potential of amino alcohol derivatives of tin as delayed action catalysts for polyurethane formation, detailed studies of the mechanism according to which the isomerization takes place is of interest.

Experimental Section

General aspects. All solvents, including deuterated solvents for NMR experiments, were dried and purified by standard procedures. All reactions were carried out under an atmosphere of dry argon using Schlenk techniques. Varian Mercury Vx 200 MHz (4-nucleus probehead), Bruker DPX-300 (5 mm WBSO probehead), Bruker Avance III HD 400 MHz, Bruker Avance III HD 500 MHz, (with Prodigy-probehead), Bruker Avance III HD 600 MHz, (with Cryo-probehead) and Agilent DD2 500 MHz spectrometers were used to obtain ^{1}H, ^{13}C NMR and the ^{119}Sn-NMR spectra as well as the 2D spectra. ^{1}H, ^{13}C, and ^{119}Sn-NMR chemical shifts are given in ppm and were referenced to $SiMe_4$ (^{1}H, ^{13}C) and $SnMe_4$ (^{119}Sn).

Melting points are uncorrected and were measured on a Büchi MP-560 device.

The electrospray ionization mass spectra were recorded on a Thermoquest-Finnigan instrument using MeOH, CH_2Cl_2 or MeCN as the mobile phase. The samples were introduced as solution via a syringe pump operating at a rate of 0.5 µL/min. The capillary voltage was 4.5 kV while the cone skimmer voltage varied between 50 and 250 kV. Identification of the expected ions was assisted by comparison of experimental and calculated isotope distribution patterns. The m/*z* values reported correspond to those of the most intense peak in the corresponding isotope pattern.

Elemental analyses were performed on a LECO-CHNS-932 analyzer under non-inert conditions.

The infrared spectra were recorded with a Perkin Elmer Two (ATR) spectrometer under non-inert conditions.

Crystallography:

Intensity data for **2**, **2a**, **8**, **9**, **9a**, **10**, **13**·C_7H_8 and **14** were collected on an XcaliburS CCD diffractometer (Oxford Diffraction) using Mo-Kα radiation at 173(2) K with an Oxford Cryostream. Intensity data for **7** were collected on an APEX-II CCD diffractometer (Bruker Corporation) using Mo-Kα radiation at 100 K. Intensity data for **13** were collected on an APEX-II CCD diffractometer (Bruker Corporation) using Mo-Kα radiation at 190 K.

The structures were solved with direct methods using SHELXS-97[36] (**2a**, **8**, **9**, **10**, **13**, **13**·C_7H_8, **14**), SIR-2004[37] (**2**), SHELXT-2014/7[38] (**7**, **9a**) and refinements were carried out against *F*2 by using SHELXL-2018/1.[36,38]

The C–H hydrogen atoms were positioned with idealized geometry and refined using a riding model. All non-hydrogen atoms were refined using anisotropic displacement parameters.

The protons of compounds **2** (OH) and **2a** (OH and NH) are located in the difference Fourier map and refined freely, distances are restrained to a fix value. The studied crystal of compound **9** was of poor quality. Consequently, the measured data set has a high R_{int} (0.1301) and in its solution the tin atom is surrounded by large residual density maxima. In the solution of the studied crystal of compound **9a** a short contact between the protons H6A and H15B is reported (1.88 Å). Since the protons are in correct calculated positions the short contact may be arised due to packing effects. In the solution of the studied crystal of compound **14** larger than expected residual density maxima outside metal atom locations are detected. To the best of our knowledge the possibilities for twinning, wrongly assigned atom types, unaccounted solvents and other model errors were eliminated.

CCDC-1858288 (**2**), CCDC-1858289 (**2a**), CCDC-1858290 (**7**), CCDC-1858291 (**8**), CCDC-1858292 (**9**), CCDC-1858293 (**9a**), CCDC-1858294 (**10**), CCDC-1858295 (**13**·C_7H_8), CCDC-1858296 (**13**) and CCDC-1858297 (**14**) contain the supplementary crystallographic data for this paper. This data can be obtained free of charge from The Cambridge Crystallographic Data Centre via www.ccdc.cam.ac.uk/data_request/cif.

For decimal rounding of numerical parameters and su values the rules of IUCr have been employed.[39]

All figures were generated using ORTEP III visualization software.[41]

Synthesis of 3-methyl[(3-methoxy-3-oxopropyl)-methylamino]propanoate MeN(CH_2CH_2COOMe)$_2$ (1a)

Methylamine (13.90 g, 447.52 mmol) was added to a solution of freshly distilled methyl acrylate (30.48 g, 354.05 mmol) in methanol (90 ml) over 30 min at 0 °C. The reaction mixture was stirred over night at ambient

10.1002/chem.201803952

temperature. The remaining volatiles were removed under reduced pressure and the compound **1a** was purified by distillation (125 °C, $6.8 \cdot 10^{-1}$ mbar) and obtained as colourless oil (46.88 g, 181.58 mmol, 51%).
^{1}H NMR (500.13 MHz, $CDCl_3$, 25 °C): δ 3.56 (s, 6H, OCH_3), 2.57 (t, ^3J(^{1}H–^{1}H) = 7.2 Hz, 4H, NCH_2), 2.34 (t, ^3J(^{1}H–^{1}H) =7.2 Hz, 4H, CH_2CH_2C(O)O), 2.11 (s, 3H, N-CH_3).
^{13}C{^{1}H} NMR (125.77 MHz, $CDCl_3$, 25 °C): δ 172.5 (s, *C*(O)O), 52.2 (s, NCH_2), 51.1 (s, OCH_3), 41.4 (s, NCH_3), 32.1 (s, NCH_2CH_2).
MS (ESI +) in CH_3CN: m/z 204.1 [**1a**+H]$^+$, 226.1 [**1a**+Na]$^+$.

Synthesis of 4,4'-(methylazanediyl)bis(2-methylbutane-2-ol) MeN($CH_2CH_2CMe_2OH$)$_2$ (1)
Compound **1a** (15.00 g, 73.81 mmol) was added dropwise to MeMgCl (23.19 g, 309.96 mmol, 4.2 eq.) in diethyl ether (500 ml) at 0 °C. Than the mixture was heated at 35 °C for 3 h, followed by subsequent addition at 0 °C of water (10.60 mL) and sodium hydroxide solution (15%, 10.60 mL). Then the mixture was stirred for 2 hat ambient temperature. The solid material that had been formed was separated by filtration and extracted with CH_2Cl_2 using a Soxhlet apparatus. The volatiles of the filtrate were removed under reduced pressure. The residue thus obtained was combined with the product obtained from the soxhlet extraction. Distillation in vacuo gave compound **1** as colourless oil (125 °C, $5.6 \cdot 10^{-1}$ mbar, 8.96 g, 44.07 mmol, 60%).
^{1}H NMR (500.13 MHz, C_6D_6, 25 °C): δ 2.41 (t, ^3J(^{1}H-^{1}H) = 6.9 Hz, 4H CH_2CH_2), 2.00 (s, 3H NCH_3), 1.49 (t,^3J(^{1}H-^{1}H)=6.9 Hz,4H, NCH_2), 1.21 (s, 12 H, CCH_3).
^{13}C{^{1}H} NMR (125.75 MHz, C_6D_6, 25 °C):δ 70.4 (s, *C*CH_3), 54.3 (s, NCH_2), 42.3 (s, NCH_3), 39.7 (s, NCH_2CH_2), 30.2 (s, CCH_3).
MS (ESI +) in CH_3CN: m/z 204.1 [**1**+H]$^+$, 186.[**1**-H_2O +H]$^+$.
IR spectroscopy (cm^{-1}): 3332 (ν_{OH}).

Synthesis of 2-[(2-hydroxy-2-methylpropyl)(methyl)amino]-2-methylpropane-1-ol MeN(CMe_2CH_2OH)(CH_2CMe_2OH) (2)
2-[(2-hydroxy-2-methylpropyl)amino]-2-methylpropan-1-ol (25 g, 156 mmol) was mixed with formic acid (21.56 g, 468 mmol,17.67 mL, 3 eq.) and formaldehyde solution (18.93 g (w = 40%), 234 mmol, 1.5 eq.) and heated at reflux for 24 h. The volatiles were removed under reduced pressure giving the ammonium formate **2a** as solid material (mp. 56 °C). It was dissolved in dichloromethane (50 mL), extracted with potassium carbonate solution (3 times 20 ml), and washed with water (20 mL). The collected organic layers were dried over sodium sulphate and filtrated. The volatiles of the filtrate were removed under reduced pressure giving 2-[(2-hydroxy-2-methylpropyl)(methyl)amino]-2-methylpropan-1-ol (22.27 g, 127.06 mmol, 81.44%) as colourless oil, which crystallized after a few days. Single crystals (mp. 53-55 °C) were obtained from its *iso*-hexane solution.
^{1}H-NMR-(2a, 300.13 MHz, $CDCl_3$, 21 °C): δ 3.37 (s, 2H, CH_2OH), 3.01 (s, 2H, NCH_2), 2.95 (s, 3H, NCH_3), 1.40 (s, 6H, C(CH_3)$_2$OH), 1.36 (s, , 6H, NC(CH_3)$_2$).
^{1}H NMR (**2,** 200.13 MHz, C_6D_6, 25 °C): δ 3.32 (s, 2H, CH_2OH), 2.39 (s, 2H, NCH_2), 2.36. (s, 3H, NCH_3), 1.21 (s, 6H, C(CH_3)$_2$OH), 1.02 (s, 6H, NC(CH_3)$_2$).
^{13}C{^{1}H} NMR-(2, 150.94 MHz, $CDCl_3$, 25 °C): δ 70.5 (s, *C*$(CH_3)_2$OH), 69.1 (s, *C*H_2OH), 60.9 (s, NCH_2), 58.2 (*s,* N*C*$(CH_3)_2$), 38.68 (s, NCH_3), 28.50 (s, C(CH_3)$_2$OH), 20.6 (s, NC(*C*H_3)$_2$).
MS (ESI +) in CH_3CN: m/z 176.1 [**2** + H]$^+$.
Elemental analysis (%) calcd for $C_9H_{21}NO_2$ (175.27 g/mol) C 61.7, H 12.1, N 8.0. Found C 61.6, H 12.1, N: 7.7.
IR spectroscopy (cm^{-1}): 3294 (ν_{OH}).

Synthesis of 2-methyl-1-(methylamino)propane-2-ol MeN(H)CH_2CMe_2OH (3a)
A mixture of methylamine (3.89 g, 41.33 mmol, 33% in ethanol) and isobutylene oxide (1.00 g, 13.87 mmol) was treated for a period of 2 h in an ultrasonic bath. The remaining volatiles were removed under reduced pressure. Compound **3a** was obtained as a colourless liquid (0.78 g, 7.56 mmol, 55%, b.p.: 85 °C (27 mbar)).
^{1}H NMR (300.13 MHz, $CDCl_3$, 25 °C): δ 2.51 (s, 3H, NCH_3), 2.49 (s, 2H, NCH_2), 1.85–2.33 (br. s, 2H, O*H*/N*H*), 1.18 (s, 6 H, CCH_3).
^{13}C{^{1}H} NMR (125.68 MHz, $CDCl_3$, 25 °C): δ 69.33 (s, $NCH_2C(CH_3)_2$), 62.69 (s, NCH_2), 37.23 (s, NCH_3), 27.42 (s, $NCH_2C(CH_3)_2$).
MS (ESI +) in CH_3CN: m/z 86.2 [**3a** – H_2O + H]$^+$, 104.1 [**3a** + H]$^+$, 145.1 [**3a** + CH_3CN + H]$^+$.

Synthesis of 3-[(2-hydroxy-2-methylpropyl)(methyl)amino] propanoate MeN(CH_2CH_2COOMe)CH_2CMe_2OH (3b)
A mixture of 2-methyl-1-(methylamino)propan-2-ol (**3a**, 5.9 g, 57.6 mmol) and methyl acrylate (4.9 g, 57.6 mmol) was treated in an ultrasonic bath for 3 h. Compound **3b** was obtained as a colourless oil in quantitative yield.
^{1}H NMR (499.78 MHz, $CDCl_3$, 25 °C): δ 3.70 (s, 3H, CH_3O), 2.84 (t, ^3J(^{1}H–^{1}H) = 7 Hz, 2H, CH_2CH_2), 2.49 (t, ^3J(^{1}H–^{1}H) = 7 Hz, 2H, NCH_2), 2.36 (s, 5H, NCH_3/NCH_2), 1.15 (s, 6 H, CCH_3).
^{13}C{^{1}H} NMR (75.47 MHz, $CDCl_3$, 25 °C): δ 173.1 (s, *C*OOCH$_3$), 69.9 (s, COO*C*H$_3$), 68.5 (s, NCH_2CH_2), 55.2 (s, NCH_2), 51.5 (s, NCH_3), 44.5 (s, NCH_2), 32.7 (s, *C*$(CH_3)_2$), 27.4 (s, CCH_3),
MS (ESI +) in CH_3CN: m/z 172.1 [**3b** - H_2O + H]$^+$, 190.1 [**3b** + H]$^+$, 212.1 [**3b** + Na]$^+$.

Synthesis of 3-[(2-hydroxy-2-methylpropyl)(methyl)amino]propan-1-ol MeN(CH_2CMe_2OH)$(CH_2)_3$OH (3)
To a stirred suspension of lithium aluminium hydride (1.19 g, 31.4 mmol) in dry THF (100 mL) was added within 15 min at 0 °C a solution of **3b** (3.09 g, 16.3 mmol) in dry THF (10 mL). After further stirring at room temperature for 3 d the solvent was removed under reduced pressure followed by addition of Et_2O (75 mL). At 0 °C H_2O (1.2 mL), 15% aqueous solution of NaOH (1.2 mL), and H_2O (3.6 mL) were subsequently added. The resulting solution was stirred for 1 h, dried with $MgSO_4$, and filtered. The solvent of the filtrate was removed under reduced pressure. Compound **3** (2.60 g, 16.08 mmol, 98%) was obtained as a colourless oil.
^{1}H NMR (300.13 MHz, $CDCl_3$, 25 °C): δ 3.82 (t, ^3J(^{1}H–^{1}H) = 6 Hz, 2H, CH_2OH), 2.72 (t, ^3J(^{1}H–^{1}H) = 6 Hz, 2H, NCH_2CH_2), 2.40 (s, 2H, N$CH_2C(CH_3)_2$), 2.38 (s, 3H, NCH_3), 1.72 (q, ^3J(^{1}H–^{1}H) = 6 Hz, 2H, $CH_2CH_2CH_2$), 1.20 (s, 6H, CCH_3).
^{13}C{^{1}H} NMR (75.47 MHz, $CDCl_3$, 25 °C): δ 70.7 (s, *C*$(CH_3)_2$OH), 69.4 (s, NCH_2CMe_2), 63.2 (s, *C*H$_2$OH), 59.5 (s, NCH_2CH_2), 45.0 (s, NCH_3), 28.8 (s, $CH_2CH_2CH_2$), 27.8 (s, C(*C*H_3)$_2$).
MS (ESI +) in CH_3CN: m/z 144.2 [**3** – H_2O + H]$^+$, 162.2 [**3** + H]$^+$.

Synthesis of 4-[(2-hydroxy-2-methylpropyl)(methyl)amino]-2-methylbutan-2-ol MeN(CH_2CMe_2OH)$CH_2CH_2CMe_2OH$ (4)
To a solution of **3b** (2.9 g, 15.5 mmol) in diethyl ether (10 mL) was added within 10 min at – 60 °C a 1.4 molar solution of methyl lithium in diethyl ether (15 mL). After the reaction mixture had been warmed to room temperature (within 20 h), the solvent was removed under reduced pressure. Water (1.5 mL) and dichloromethane (10 mL) was added. After stirring of the solution for 1 h, drying of the latter with $MgSO_4$ and subsequent filtration, the reaction mixture was extracted with dichloromethane (250 mL). Distillation under reduced pressure (90 °C, $4 \cdot 10^{-2}$ mbar) gave compound **4** (1.97 g, 10.4 mmol, 67%) as a light yellowish oil.
^{1}H NMR (500.13 MHz, $CDCl_3$, 25°C): δ 2.77 (t, ^3J(^{1}H–^{1}H) = 5 Hz, 2H, NCH_2CH_2), 2.43 (s, 2H, N$CH_2C(CH_3)_2$), 2.40 (s, 3H, NCH_3), 1.65 (t, ^3J(^{1}H–^{1}H) = 5 Hz, 2H, NCH_2CH_2), 1.25 (s, 6H, $NCH_2CH_2C(CH_3)_2$), 1.20 (s, 6H, $NCH_2C(CH_3)_2$).
^{13}C{^{1}H} NMR (125.77 MHz, $CDCl_3$, 25°C): δ 71.6 (s, $NCH_2CH_2C(CH_3)_2OH$), 70.6 (s, $NCH_2C(CH_3)_2OH$), 69.7 (s, $NCH_2(CH_3)_2$), 57.2 (s, NCH_2CH_2), 45.5 (s, NCH_3), 38.0 (s, NCH_2CH_2), 29.8 (s, $CH_2CH_2C(CH_3)_2$), 27.8 (s, $NCH_2C(CH_3)_2$).
MS (ESI +) in CH_3CN: m/z 172.2 [**4** – H_2O + H]$^+$, 190.2 [**4** + H]$^+$.

Synthesis of 3-[(2-hydroxyethyl)(methyl)amino]propanoate MeN(CH_2CH_2OH)CH_2CH_2COOMe (5a)
A mixture of 2-methylaminoethanol (17.6 g, 234.5 mmol) and methyl acrylate (20.2 g, 234.2 mmol) was treated in an ultrasonic bath for 3 h. Compound **5a** was obtained as a colourless oil in almost quantitative yield.
^{1}H NMR (300.13 MHz, $CDCl_3$, 25 °C): δ 3.68 (s, 3 H, COOCH_3), 3.58 (t, ^3J(^{1}H–^{1}H) = 6 Hz, 2H, CH_2CH_2OH), 2.73 (t, ^3J(^{1}H–^{1}H) = 6 Hz, 2H, NCH_2CH_2COO), 2.53 (t, ^3J(^{1}H–^{1}H) = 5 Hz, 4H, NCH_2CH_2OH), 2.48 (t, ^3J(^{1}H–^{1}H) = 7 Hz, 2H, NCH_2CH_2COO), 2.26 (s, 3 H, NCH_3).
^{13}C{^{1}H} NMR (75.47 MHz, $CDCl_3$, 25 °C): δ 173.0 (s, *C*OOCH$_3$), 58.7 (s, COOCH$_3$), 58.4 (s, CH_2OH), 52.3 (s, NCH_2), 51.6 (s, NCH_2), 41.6 (s, NCH_3), 32.4 (s, *C*H$_2$COOCH$_3$),
MS (ESI +) in CH_3CN: m/z 144.1 [**5a** + H_2O + H]$^+$, 162.1 [**5a** + H]$^+$, 184.0 [**5a** + Na]$^+$.

Synthesis of 4-[(2-hydroxyethyl)(methyl)amino]-2-methylbutan-2-ol (5)
To a solution of **5a** (2.2 g, 13.6 mmol) in diethylether (20 mL) was added within 10 min at – 60 °C of a 1.4 molar solution of methyl lithium in diethylether (30 mL). After the reaction mixture had been warmed to room temperature (within 20 h), the solvent was removed under reduced pressure. Water (1.5 mL) and dichloromethane (10 mL) were added. After stirring of the solution for 1 h, drying of the latter with $MgSO_4$ and subsequent filtration, the reaction mixture was extracted with dichloromethane (250 mL). Distillation under reduced pressure (90 °C, $4 \cdot 10^{-2}$ mbar) gave compound **5** (0.26 g, 1.59 mmol, 24%) as a light yellowish oil.

^{1}H NMR (300.13 MHz, $CDCl_3$, 25 °C): δ 3.70 (t, $^3J(^1H–^1H)$ = 6 Hz, 2H, NCH_2CH_2OH), 2.5 – 2.7 (not resolved, 4H, NCH_2), 2.32 (s, 3H, NCH_3), 1.64 (t, $^3J(^1H–^1H)$ = 6 Hz, 2H, $CH_2C(CH_3)_2OH$), 1.24 (s, 6H, $C(CH_3)_2$),
^{13}C{^{1}H} NMR (125.68 MHz, $CDCl_3$, 25 °C): δ 71.26 (s, $NCH_2CH_2CMe_2OH$), 59.75 (s, NCH_2CH_2OH), 59.55 (s, NCH_2CH_2OH), 54.52 (s, $NCH_2CH_2C(CH_3)_2$), 42.39 (s, NCH_3), 37.74 (s, $NCH_2CH_2C(CH_3)_2$), 29.63 (s, $C(CH_3)_2$).
MS (ESI +) in CH_3CN: m/z 146.1 [**5** – H_2O + H]$^+$, 162.1 [**5** + H]$^+$, 198.1 [**5** + 2 H_2O + H]$^+$.

Synthesis of 3-[(2-hydroxyethyl)(methyl)amino]propan-1-ol MeN(CH_2CH_2OH)(CH_2)$_3$OH (6)
A magnetically stirred suspension of 2-methylaminoethanol (5.0 g, 66.6 mmol), 3-chloro-1-propanol (6.3 g, 66.6 mmol) and potassium carbonate (9.2 g, 66.6 mmol) in acetonitrile (40 mL) was heated at reflux for a period of 5 d. The reaction mixture was filtrated, and the volatiles of the filtrate were removed under reduced pressure. Compound **6** was obtained as a colourless oil (7.5 g, 56.3 mmol, 85%, b.p.: 140 °C (27 mbar)).
^{1}H NMR (300.13 MHz, $CDCl_3$, 25 °C): δ 3.85 (t, $^3J(^1H–^1H)$ = 6 Hz, 2H, CH_2OH), 3.68 (t, $^3J(^1H–^1H)$ = 6 Hz, 2H, CH_2OH), 3.23 (br. s, 2H, OH), 2.63 (t, $^3J(^1H–^1H)$ = 6 Hz, 2H, NCH_2), 2.56 (t, $^3J(^1H–^1H)$ = 6 Hz, 2H, NCH_2), 2.30 (s, 3H, NCH_3), 1.69–1.77 (m, 2H, $CH_2CH_2CH_2$).
^{13}C{^{1}H} NMR (75.47 MHz, $CDCl_3$, 25 °C): δ 62.8 (s, NCH_2), 59.5 (s, CH_2OH), 59.1 (s, CH_2OH), 56.7 (s, NCH_2), 42.1 (s, NCH_3), 28.4 (s, $CH_2CH_2CH_2$).
MS (ESI +) in CH_3CN: m/z 134.1 [**6** + H]$^+$, 156.0 [**6** + Na]$^+$, 192.1 [**6** + CH_3CN + H_3O]$^+$.

Synthesis of *spiro*-[*n*BuN($CH_2CMe_2O)_2$]$_2$Sn (7)
$Sn(Ot\text{-}Bu)_4$ (30.02 g, 73.00 mmol) was dissolved in toluene (900 mL) and a solution of *n*-BuMeN($CH_2CMe_2OH)_2$, **B,** (30.15 g, 130.70 mmol) in toluene (200 mL) was added dropwise over a period of 15 min. The reaction mixture was heated to reflux for 2 h, and the toluene/*tert*-butanol azeotrope was removed by distillation. Colourless crystals of **7** (40.00 g, 72.81 mmol, 99.7%, mp: 180 °C) were obtained from its concentrated toluene solution.
^{1}H NMR (600.29 MHz, C_6D_6, 22 °C): δ 2.43 (s, 8H, $NCH_2C(CH_3)_2$), 2.35 (m, 4H, NCH_2), 1.31, 1.26, 1.18 and 1.10 (m, 8H, CH_2), 1.14 (s, 24H, CCH_3), 0.87 and 0.84 (t, $^3J(^1H–^1H)$ 7.33 Hz, 6H, CH_2CH_3).
^{13}C{^{1}H} NMR (150.94 MHz, C_6D_6, 25 °C): δ 71.3 (s, $C(CH_3)_2$), 69.1 (s, $NCH_2C(CH_3)_2$), 60.6 (s, NCH_2), 33.9 (s, CH_2), 28.6 (s, $C(CH_3)_2$), 25.4 (s, CH_2), 21.4, 21.22 (s, CH_2CH_3). Tin satellites are not resolved.
^{119}Sn{^{1}H} NMR (149.26 MHz, C_6D_6, 25 °C): δ –437.
MS (ESI +) in CH_3CN: m/z = 218.1 [**B**+H]$^+$, 551.3 [**7** +H]$^+$, 573.4 [**7**+Na]$^+$, 589.4 [**7**+K]$^+$, 614.4 [**7**+MeCN + H]$^+$.
Elemental analysis (%) calcd for $C_{24}H_{50}N_2O_4Sn$ + 0.5·H_2O (558.78 g/mol) C 51.6, H 9.2, N 5.0. Found C 51.4, H 9.0, N: 5.0. Because the measurement was performed under non-inert conditions, the compound partially hydrolysed.

Synthesis of *spiro*-[MeN($CH_2CH_2CMe_2O)_2$]$_2$Sn (8)
$Sn(Ot\text{-}Bu)_4$ (1.03 g, 2.51 mmol) was dissolved in toluene (150 mL) and a solution of **1**, MeN($CH_2CH_2CMe_2OH)_2$, (1.00 g, 4.92 mmol) in toluene (30 mL) was added dropwise over a period of 5 min. The reaction mixture was heated to reflux for 1 h, and the toluene/*tert*-butanol azeotrope was removed by distillation. Colourless crystals of **8** (mp: 180 °C, 1.60 g, 3.07 mmol, 31%) were obtained from its concentrated toluene solution at 4 °C.
^{1}H NMR (400.25 MHz, C_6D_6, 25 °C): δ 2.39 (t, $^3J(^1H\text{-}^1H)$= 6.6 Hz, 8H, NCH_2), 1.99 (s, 6H, NCH_3), 1.47 (t, $^3J(^1H\text{-}^1H)$= 6.8 Hz, 8H, NCH_2CH_2), 1.19 (s, 24H, $C(CH_3)_2$).
^{13}C{^{1}H} NMR-(100.46 MHz, , C_6D_6, 25 °C): δ 70,5 (s, $C(CH_3)_2$), 54.5 (s, NCH_2), 42.4 (s, NCH_3), 39.8 (s, NCH_2CH_2), 30.4 (s, $C(CH_3)_2$).
^{119}Sn{^{1}H} NMR-(150.94 MHz, CD_2Cl_2, 25 °C): δ –603.
MS (ESI –) in CH_3CN: m/z 138.0 [**8** + Cl]$^-$.

Synthesis of *spiro*-[*p*-$FC_6H_4N(CH_2CMe_2O)_2$]$_2$Sn (9)
$Sn(Ot\text{-}Bu)_4$ (2.01 g, 4.86 mmol) was dissolved in toluene (100 mL) and a solution of *p*-$FC_6H_4N(CH_2CMe_2OH)_2$, **C**, (2.42 g, 9.49 mmol) in toluene (50 mL) was added dropwise over a period of 10 min. The reaction mixture was heated to reflux for 1 h, and the toluene/*tert*-butanol azeotrope was removed by distillation. After filtration the filtrate was concentrated to a volume of approximately 50 mL and stored at 4 °C. Yellow crystals of **9** (1.88 g, 3.19 mmol, 65%) were obtained (mp.: 193-194 °C).
^{1}H NMR (600.29 MHz, C_6D_6, 25 °C): δ 7.91–7.87(m, 4H, FC(CH)$_2$), 6.77–6.72 (m, 4H, NC(CH)$_2$), 3.37, 2.97 (d, $^4J(^1H–^1H)$ = 11.74 Hz, 2H, NCH_2), 3.07, (s, 4H, 2 x NCH_2), 1.55, 1.30 (s, 6H, CH_3), 0.78 (s, 12H, CH_3).
^{13}C{^{1}H} NMR (150.94 MHz, C_6D_6, 25 °C): δ 163.0, 161.3 (s, *C*F), 146.70, 146.68 (s, *C*N), 129.81, 129.76 (s, H*C*CF), 116.6, 116.5 (s, H*C*CN), 71.9, 71.1 (s, CH_2), 68.9, 68.4 (s, *C*OSn), 33.8, 33.5, 31.4, 31.2 (s, CH_3).
^{19}F NMR (376.61 MHz, C_6D_6, 25 °C): δ –113.62.
^{119}Sn{^{1}H} NMR (149.26 MHz, C_6D_6, 25 °C): δ –447.
9 is not stable under ESI MS conditions.
Elemental analysis (%) calcd for $C_{28}H_{40}F_2N_2O_4Sn_2$ + 0.5 H_2O (633.3 g/mol): C 53.0, H 6.5, N 4.4. Found: 53.0, 6.5, 4.2. The measurement was performed under non-inert conditions. Partial hydrolysis took place.

***p*-$FC_6H_4N(CH_2CMe_2O)_2Sn(Ot\text{-}Bu)_2$ 9a**
Compound 9a was obtained as by-product in the synthesis of **9**.
^{19}F NMR (376.61 MHz, C_6D_6, 25 °C): δ –116.42.
^{119}Sn{^{1}H} NMR (149.26 MHz, C_6D_6, 25 °C): δ –402 (23%), –447 (**9**, 77%).

Synthesis of *spiro*–[MeN($CH_2CMe_2O)(CMe_2CH_2O)$]$_2$Sn (10)
$Sn(Ot\text{-}Bu)_4$ (2.60 g, 6.33 mmol) was dissolved in toluene (150 mL) and a solution of MeN($CH_2CMe_2OH)(CMe_2CH_2OH)$, **2**, (2.16 g, 12.34 mmol,) in toluene (50 mL) was added dropwise over a period of 15 min. The reaction mixture was heated to reflux for 1 h, and the toluene/*tert*-butanol azeotrope was removed by distillation. The reaction mixture was concentrated to a volume of approximately 50 mL and stored at 4 °C. Colourless crystals of **10** (2.17 g, 4.66 mmol, 74%) were obtained (mp. 186 °C).
^{1}H-NMR (400.25 MHz, C_6D_6, 25 °C): δ 3.69 and 3.47 (AX, $^3J(^1H–^1H)$ = 10.8 Hz, 2H, OCH_2), 3.68 and 3.51 (AX, $^3J(^1H–^1H)$ = 11.3 Hz, 2H, OCH_2), 2.38 and 1.77 (AX, $^3J(^1H–^1H)$ = 12.7 Hz, 2H, NCH_2), 2.37 and 1.72 (AX, $^3J(^1H–^1H)$ = 12.7 Hz, 2H, NCH_2), 2.27 and 2.26 (s, 6H each, NCH_3), 1.53, 1.36, 1.30 and 1.27 (s, 6H each, $OC(CH_3)_2$), 1.19, 1.04, 0.61 and 0.58 (s, 6H each, $NC(CH_3)_2$). Two Isomers in solution.
^{13}C{^{1}H}-NMR (100.64 MHz, C_6D_6, 25 °C) δ 70. 1 (s, $J(^{117/119}Sn)$ = 23 Hz, $C(CH_3)_2$), 69.6 (s, $J(^{117/119}Sn)$ = 27 Hz, $C(CH_3)_2$), 67.6 (s, OCH_2), 67.5 (s, OCH_2), 61.3 (s, $J(^{117/119}Sn)$ = 48 Hz, NCH_2), 61.1 (s, $J(^{117/119}Sn)$ = 52 Hz, NCH_2), 40.0 (s, NCH_3), 39.4 (s, NCH_3), 34.1, 33.8, 32.0 and 31.1 (s, $OC(CH_3)_2$), 24.9, 24.7, 18.1 and 17.6 (s, $NC(CH_3)_2$).
^{119}Sn{^{1}H}-NMR (sample from the crude reaction mixture**,** 194.26 MHz, C_6D_6, 22 °C) δ = –398, –437, –443, –460, –500.
^{119}Sn{^{1}H}-NMR (149.26 MHz, C_6D_6, 25 °C): δ –437 (40%), –443 (60%).
^{119}Sn{^{1}H}-NMR (149.26 MHz, $CDCl_3$, 25 °C): δ –445.
^{119}Sn{^{1}H}-NMR (149.26 MHz, CD_2Cl_2, 25 °C): δ –438 (br.$\nu_{1/2}$ = 150 Hz, 38%), –443 (62%).
^{119}Sn{^{1}H}-NMR (149.26 MHz, CH_3CN, 25 °C): δ –438 (br.$\nu_{1/2}$ = 134 Hz, 45%), –443 (55%).
^{119}Sn{^{1}H}-NMR (149.26 MHz, acetone–d_8, 25 °C): δ –445.
^{119}Sn{^{1}H}-NMR (149.26 MHz, tetracholormethane-d_2, 25 °C): δ –446 (70%), –443 (18%), -454 (12%).
MS (ESI +) in CH_3CN: m/z 467.2 [**10** + H]$^+$.
Elemental analysis (%) calcd for $C_{18}H_{38}N_2O_4Sn$ + 1H_2O (483.2 g/mol): C 44.7, H 8.3, N 5.8. Found: 44.5, 7.9, 6.6. The measurement was performed under non-inert conditions. Partial hydrolysis took place.

Synthesis of spiro–[MeN($CH_2CH_2CH_2O)(CH_2CMe_2O)$]$_2$Sn (11)
To a stirred solution of $Sn(Ot\text{-}Bu)_4$ (1.9 g, 4.55 mmol) in dry toluene (75 mL) was added within 10 min at room temperature a solution of **3** (1.5 g, 9.1 mmol) in 25 mL dry toluene. The solution was stirred for 30 min followed by distillation of the toluene/tert-butanol azeotrope and complete removal in vacuo of all volatiles Compound **11** (1.2 g, 2.7 mmol, 59%) was obtained as a waxy residue.
^{1}H NMR (300.13 MHz, C_6D_6, 25 °C): δ 5.04–4.94 (m), 4.69 – 4.80 (m), 3.83 (t, ^3J = 6 Hz), 3.31 – 3.47 (m), 2.47 – 2.70 (m), 2.44 (s), 2.32 – 2.42 (m), 2.22 (s), 2.17 (s), 2.11 (s), 1.81 – 1.94 (m), 1.43 (s), 1.60 (q, J = 6 Hz), 1.37 (s), 1.33 (s), 1.30 (s), 1.29 (s), 1.22 (s). Given the existence of several isomers in solution, no assignment of the resonances was done.
^{13}C{^{1}H} NMR (75.47 MHz, $CDCl_3$): δ 70.9 (s), 70.5 (s), 69.3 (s), 67.1 (s), 66.3 (s), 65.8 (s), 62.7 (s), 59.1 (s), 44.9 (s), 42.0 (s), 34.2 (s), 33.7 (s), 32.2 (s), 29.1 (s), 29.0 (s), 27.8 (s). Given the existence of several isomers in solution, no assignment of the resonances was done.
^{119}Sn{^{1}H} NMR (111.92 MHz, C_6D_6, 25 °C): δ (ppm) = –512 (s, Integral 48%), –512 (s, Integral 46%), –515 (s, Integral 6 %).
Elemental analysis (%) calcd for $C_{16}H_{34}N_2O_4Sn$ + H_2O (455.18 g/mol): C, 42.2; H, 8.0; N, 6.2. Found: C, 42.7; H, 8.1; N, 6.0.
MS (ESI+) (CH_3CN, m/z): 162.1 [**3** + H]$^+$, 439.1 [**11** + H]$^+$.

Synthesis of *spiro*-[MeN($CH_2CH_2CMe_2O)$ ($CH_2CMe_2O)$]$_2$Sn (12)
To a stirred solution of $Sn(Ot\text{-}Bu)_4$ (1.5 g, 3.6 mmol) in dry toluene (100 mL) was added within 10 min at room temperature a solution of **4** (1.4 g, 7.1 mmol) in 20 ml dry toluene. The solution was stirred for 30 min followed by distillation of the toluene/tert-butanol azeotrope and complete removal

in vacuo of all volatiles. Compound **12** (1.2 g, 2.3 mmol, 65%) was obtained as a waxy residue.
^{1}H NMR (300.13 MHz, $CDCl_3$, 25 °C): δ 7.12 – 7.24 (m), 3.49 – 3.73 (m), 3.12 – 3.36 (m), 2.54 – 2.85 (m), 2.50 (s), 2.41 (s), 2.03 – 2.39 (m), 1.88 (t, ^3J = 15 Hz), 1.09 – 1.57 (m), 0.80 – 0.91 (m). Given the existence of several isomers in solution, no assignment of the resonances was done.
^{13}C{^{1}H} NMR (75.47 MHz, $CDCl_3$, 25 °C): δ 129.0 (s), 128.2 (s), 125.3 (s), 74.6 (s), 69.6 (s), 67.6 (s), 67.5 (s), 57.9 (s), 42.3 (s), 37.2 (s), 35.9 (s), 34.8 (s), 32.7 (s), 30.2 (s), 29.8 (s), 27.8 (s), 21.4 (s). Given the existence of several isomers in solution, no assignment of the resonances was done.
^{119}Sn{^{1}H} NMR (111.92 MHz, $CDCl_3$, 25 °C): δ –529 (s, Integral 66%), –532 (s, Integral 13%), –555 (s, Integral 21%).
Elemental analysis (%) calcd for $C_{20}H_{42}N_2O_4Sn$ (493.27 g/mol): C, 48.7; H, 8.6; N, 5.7. Found: C, 43.0; H, 8.1; N, 4.5. The measurement was done under non-inert conditions. Apparantly, partial hydrolysis has taken place.
MS (ESI+) (CH_3CN, m/z): 190.1 [**4** + H]$^+$. **12** is not stable under ESI-MS conditions.

Synthesis of spiro-[MeN($CH_2CH_2CMe_2O$)(CH_2CH_2O)]$_2$Sn (13)
To a stirred solution of Sn(O*t*-Bu)$_4$ (1.6 g, 4.55 mmol) in dry toluene (100 mL) was added within 15 min at room temperature a solution of **5** (1.3 g, 8.1 mmol) in dry toluene (25 mL). The solution was stirred for 30 min followed by distillation of the toluene/tert-butanol azeotrope and complete removal in vacuo of all volatiles Compound **13** (0.5 g, 1.1 mmol, 29%) was obtained as colourless solid. Single crystals were obtained from its toluene solution at – 10 °C.
^{1}H NMR (300.13 MHz, $CDCl_3$, 25 °C): δ 5.70 (s, ligand-O*H*), 4.08 – 4.18 (m), 3.94 – 4.04 (m), 3.69 (t, J = 5 Hz), 3.79 – 3.88 (m), 3.43 – 3.55 (m), 3.05 – 3.36 (m), 2.93 – 3.03 (m), 2.75 (s), 2.60 – 2.69 (m), 2.58 (s), 2.55 (s), 2.19 – 2.53 (m), 1.81 – 2.09 (m), 1.49 – 1.63 (m), 1.45 (s), 1.31 (s), 1.26 (s), 1.25 (s), 1.21 (s), 1.10 (s). Given the existence of several isomers in solution, no assignment of the resonances was done.
^{13}C{^{1}H} NMR (125.68 MHz, $CDCl_3$, 25 °C): δ 73.60 (s), 72.70 (s), 70.96 (s), 61.37 (s), 59.81 (s), 59.62 (s), 59.53 (s), 58.19 (s), 57.13 (s), 56.98 (s), 56.33 (s), 54.50 (s), 53.33 (s), 44.49 (s), 42. 50 (s), 37.79 (s), 37.74 (s), 37.25 (s), 37.13 (s), 34.73 (s), 32.33 (s), 31.40 (s), 29.68 (s), 29.39 (s). Given the existence of several isomers in solution, no assignment of the resonances was done.
^{119}Sn{^{1}H} NMR (111.92 MHz, C_6D_6, 25 °C): δ –513 (s, Integral 35%), –556 (bs, $\nu_{1/2}$ = 150 Hz, Integral 65%).
Elemental analysis (%) calcd for $C_{16}H_{34}N_2O_4Sn$ (437.16 g/mol): C, 44.0; H, 7.8; N, 6.4. Found: C, 43.6; H, 7.7; N, 6.3.
MS (ESI+) (CH_3CN, m/z): 162.1 [**5** + H]$^+$, 539.2 [**13** + 2 CH_3CN + H_2O + H]$^+$.

Synthesis of spiro-[MeN(CH_2CH_2O) ($CH_2CH_2CH_2O$)]$_2$Sn (14)
To a stirred solution of Sn(O*t*-Bu)$_4$ (2.6 g, 6.4 mmol) in dry toluene (80 mL) was added within 15 min at room temperature a solution of **6** (1.7 g, 12.8 mmol) in 40 ml dry toluene. The solution was stirred for 30 min followed by distillation of the toluene/tert-butanol azeotrope and complete removal in vacuo of all volatiles. Compound **14** (1.11 g, 2.9 mmol, 45%) was obtained as colourless solid. Single crystals were obtained from its toluene solution at –10 °C.
^{1}H NMR (300.13 MHz, $CDCl_3$, 25 °C): δ 7.08 – 7.23 (m), 4.24 – 4.45 (m), 4.02 – 4.23 (m), 3.63 – 4.00 (m), 3.32 – 3.56 (m), 2.80 – 3.11 (m), 2.64 (s), 2.62 (s), 2.59 (s), 2.56 (s), 2.11 – 2.52 (m), 1.35 – 1.50 (m), 1.20 (s). Given the existence of several isomers in solution, no assignment of the resonances was done.
^{13}C{^{1}H} NMR (75.47 MHz, $CDCl_3$, 25 °C): δ (ppm) = 28.91 (s), 29.03 (s), 29.16 (s), 39.11 (s), 39.34 (s), 39.70 (s), 39.94 (s), 61.58 (s), 61.64 (s), 61.82 (s), 62.02 (s), 62.18 (s), 62.41 (s), 62.68 (s), 62.87 (s), 64.90 (s), 65.62 (s), 65.62 (s), 66.29 (s). Given the existence of several isomers in solution, no assignment of the resonances was done.
^{119}Sn{^{1}H} NMR (111.92 MHz, $CDCl_3$, 25 °C): δ (ppm) = –516 (s, Integral 47 %), –524 (s, Integral 30 %), –525 (s, Integral 23 %).
Elemental analysis (%) calcd for $C_{12}H_{26}N_2O_4Sn$ (381.06 g/mol): C, 37.8; H, 6.9; N, 7.4. Found: C, 37.2; H, 7.4; N, 7.1.
MS (ESI+) (CH_3CN, m/z): 134.1 [**6** + H]$^+$, 383.1 [**14** + H]$^+$.

Computational Details
The DFT calculations were performed with Gaussian09[23] by using the hybrid functional B3LYP[24–26], the pure BP86[24,27] functional and the wB97xD[28] functional. The latter includes dispersive interactions. The split valence basis set def2-TZVP[29,30] was used. For the tin atom it contains the effective core potentials. Followed the geometry optimization, stationary points were verified by frequency analysis (no imaginary frequencies for local minima). For the calculations including toluene as solvent the IEFPCM solvent model was used.[31–35]

Acknowledgements

We thank Mrs. S. Marzian for recording the ESI mass spectra, Mr. M. Hüffner for performing the elemental analyses, and Mrs. H. Schulte for conducting powder XRD measurements.

This work contains part of the PhD thesis of Britta Glowacki, TU Dortmund 2018.

Keywords: tin • amino alcohol • DFT calculation • X-ray crystallography • ^{119}Sn NMR spectroscopy

Literature

[1] a) R. C. Mehrotra, V. D. Gupta, *Indian J. Chem.* **1967**, *5*, 643. b) A. Tzschach, M. Scheer, K. Jurkschat, *Z. anorg. allg. Chem.* **1984**, 147; c) A. Zschunke, C. Mügge, M. Scheer, K. Jurkschat, A. Tzschach, *J. Crystallogr. Spectr. Res.* **1983**, *13*, 201; d) A. Zschunke, M. Scheer, M. Völtzke, K. Jurkschat, A. Tzschach, *J. Organomet. Chem.* **1986**, 325.
[2] a) J. G. Verkade, *Coord. Chem. Rev.* **1994**, *137*, 233; b) S. S. Karlova, D. A. Tyurina, M. V. Zabalova, G. S. Zaitseva, *J. Mol. Struct* **2005**, 31; c) K. Jurkschat, C. Mügge, A. Tzschach, A. Zschunke, G. Engehardt, E. Lippmaa, M. Mägi, *J. Organomet. Chem.* **1979**, 301.
[3] a) WHO, *Inorganic Tin in Drinking-Water*, Geneva, **2004**; b) IPCS, *Tin and Organotin Compounds*. Inter-Organization Programme for the Sound Management of Chemicals, International Programme on Chemical Safety, World Health Organization, Geneva, **2005**; c) IPCS, *Tin and Organotin Compounds. A Preliminary Review*. International Programme on Chemical Safety, World Health Organization, Geneva, **1980**; d) European Food Safety Authority, *EFSA Journal* **2005**, 1.
[4] a) T. Zöller, K. Jurkschat, *Inorg. Chem.* **2013**, *52*, 1872; b) T. Zöller, C. Dietz, L. Iovkova-Berends, O. Karsten, G. Bradtmöller, A.-K. Wiegand, Y. Wang, V. Jouikov, K. Jurkschat, *Inorg. Chem.* **2012**, *51*, 1041; c) B. Glowacki, M. Lutter, D. Schollmeyer, W. Hiller, K. Jurkschat, *Inorg. Chem.* **2016**, *55*, 10218; d) L. Iovkova-Berends, T. Berends, C. Dietz, G. Bradtmöller, D. Schollmeyer, K. Jurkschat, *Eur. J. Inorg. Chem.* **2011**, *24*, 3632; e) L. Iovkova-Berends, T. Berends, T. Zöller, G. Bradtmöller, S. Herres-Pawlis, K. Jurkschat, *Eur. J. Inorg. Chem.* **2012**, *19*, 3191; f) T. Zöller, L. Iovkova-Berends, T. Berends, C. Dietz, G. Bradtmöller, K. Jurkschat, *Inorg. Chem.* **2011**, *50*, 8645; g) T. Zöller, L. Iovkova-Berends, C. Dietz, T. Berends, K. Jurkschat, *Chem. Eur. J.* **2011**, *17*, 2361.
[5] B. Glowacki, M. Lutter, H. Alnasr, R. Seymen, W. Hiller, K. Jurkschat, *Inorg. Chem.* **2017**, 4937.
[6] L. Iovkova-Berends, T. Berends, T. Zöller, D. Schollmeyer, G. Bradtmöller, K. Jurkschat, *Eur. J. Inorg. Chem.* **2012**, *21*, 3463.
[7] K. Jurkschat, J. Kalbitz, M. Dargatz, E. Kleinpeter, A. Tzschach, *J. Organomet. Chem.* **1988**, *347*, 41.
[8] K. Jurkschat, C. Klaus, M. Dargatz, A. Tzschach, J. Meunier-Piret, B. Mathieu, *Z. anorg. allg. Chem.* **1989**, 122.
[9] M. Lutter, L. Iovkova-Berends, C. Dietz, V. Jouikov, K. Jurkschat, *Main Group Met. Chem.* **2012**, *35*.
[10] a) J. Krause, S. Richter, S. Lindner, A. Schmidt, K. Jurkschat, M. Schürmann, G. Bradtmöller, DE102008021980 A1, **2009**; b) K. Jurkschat, L. Iovkova-Bernds, T. Zöller, M. Schürmann, WO2011113926 A1, **2011**.
[11] F. Richter, K. Jurkschat, L. Iovkova-Berends, T. Zöller, EP2772496 A1, **2014**.
[12] F. Richter, K. Jurkschat, M. Wagner, V. Abeyawarathan, M. Gock, EP2990381 A1, **2016**.
[13] a) Z. Wang, *Comprehensive Organic Name Reactions and Reagents*, John Wiley & Sons, Inc, Hoboken, NJ, USA, **2010**; b) W. Eschweiler, *Ber. Dtsch. Chem. Ges.* **1905**, *38*, 880; c) H. T.

Clarke, H. B. Gillespie, S. Z. Weisshaus, *J. Am. Chem. Soc.* **1933**, *55*, 4571.
[14] J. Grell, J. Bernstein, G. Tinhofer, *Acta Cryst.* **1999**, 1030.
[15] J. Bernstein, R. E. Davis, L. Shimoni, N.-L. Chang, *Angew. Chem. Int. Ed.* **1995**, 1555.
[16] T. Zöller, *Dissertation,* **2014**, Technische Universität Dortmund.
[17] U. Kolb, M. Draeger, M. Dargatz, K. Jurkschat, *Organometallics* **1995**, *14*, 2827.
[18] G. S. Pawley, *J Appl Crystallogr* **1981**, *14*, 357.
[19] R. S. Berry, *J. Chem. Physics* **1960**, *32*, 933.
[20] A. Rodger, B. F. G. Johnson, *Inorg. Chem.* **1988**, *27*, 3061.
[21] K. V. Zaitsev, S S. Karlov, A. A. Selina, Yu. F. Oprunenko, A. V. Churakov, B. Neumüller, J. A. K. Howard, G. S. Zaitseva, *Eur. J. Inorg. Chem.* **2006**, 1987.
[22] J. D. Kennedy, W. McFarlane, G. S. Pyne, *Bull. Soc. Chim. Belg.* **1975**, *84*, 298.
[23] M. J. Frisch, G. W. Trucks, H. B. Schlegel, G. E. Scuseria, M. A. Robb, J. R. Cheeseman, G. Scalmani, V. Barone, G. A. Petersson, H. Nakatsuji, X. Li, M. Caricato, A. Marenich, J. Bloino, B. G. Janesko, R. Gomperts, B. Mennucci, H. P. Hratchian, J. V. Ortiz, A. F. Izmaylov, J. L. Sonnenberg, D. Williams-Young, F. Ding, F. Lipparini, F. Egidi, J. Goings, B. Peng, A. Petrone, T. Henderson, D. Ranasinghe, V. G. Zakrzewski, J. Gao, N. Rega, G. Zheng, W. Liang, M. Hada, M. Ehara, K. Toyota, R. Fukuda, J. Hasegawa, M. Ishida, T. Nakajima, Y. Honda, O. Kitao, H. Nakai, T. Vreven, K. Throssell, J. A. Montgomery, Jr., J. E. Peralta, F. Ogliaro, M. Bearpark, J. J. Heyd, E. Brothers, K. N. Kudin, V. N. Staroverov, T. Keith, R. Kobayashi, J. Normand, K. Raghavachari, A. Rendell, J. C. Burant, S. S. Iyengar, J. Tomasi, M. Cossi, J. M. Millam, M. Klene, C. Adamo, R. Cammi, J. W. Ochterski, R. L. Martin, K. Morokuma, O. Farkas, J. B. Foresman, D. J. Fox, *Gaussian 09, Revision E.01*, Gaussian, Inc., Wallingford CT, **2013**.
[24] A. D. Becke, *J. Chem. Phys.* **1993**, *98*, 5648.
[25] C. Lee, W. Yang, R. G. Parr, *Phys. Rev. B* **1988**, *37*, 785.
[26] A. D. Becke, *Phys. Rev. A* **1988**, *38*, 3098.
[27] J. P. Perdew, *Phys. Rev. B* **1986**, *33*, 8822.
[28] J.-D. Chai, M. Head-Gordon, *Phys. Chem. Chem. Phys.* **2008**, *10*, 6615.
[29] F. Weigend, R. Ahlrichs, *Phys. Chem. Chem. Phys.* **2005**, *7*, 3297.
[30] B. Metz, H. Stoll, M. Dolg, *J. Chem. Phys.* **2000**, *113*, 2563.
[31] E. Cancès, B. Mennucci, J. Tomasi, *J. Chem. Phys.* **1997**, *107*, 3032.
[32] B. Mennucci, E. Cancès, J. Tomasi, *J. Phys. Chem. B* **1997**, *101*, 10506.
[33] S. Miertuš, E. Scrocco, J. Tomasi, *Chem. Phys.* **1981**, *55*, 117.
[34] R. Cammi, J. Tomasi, *J. Comput. Chem.* **1995**, *16*, 1449.
[35] J. Tomasi, B. Mennucci, R. Cammi, *Chem. Rev.* **2005**, *105*, 2999.
[36] G. Sheldrick, *Acta Cryst.* **2008**, 112.
[37] M. C. Burla, R. Caliandro, M. Camalli, B. Carrozzini, G. L. Cascarano, L. de Caro, C. Giacovazzo, G. Polidori, R. Spagna, *J. Appl. Crystallogr.* **2005**, *38*, 381.
[38] G. Sheldrick, *Acta Cryst.* **2015**, 3.
[39] W. Clegg, *Acta Cryst.* **2003**, e2.
[40] a) L. J. Farrugia, *J. Appl. Cryst.* **1997**, *30*, 565; b) L. J. Farrugia, *J. Appl. Cryst.* **2012**, *45*, 849.
[41] a) L. J. Farrugia, *J. Appl. Cryst.* **2012**, 849; b) L. J. Farrugia, *J. Appl. Cryst.* **1997**, 565.

10.1002/chem.201803952

WILEY-VCH

Entry for the Table of Contents (Please choose one layout)

Layout 1:

FULL PAPER

The length of the amino alcoholate chains as well as the identity of the substituents at the side chains and the nitrogen atoms control the geometrical environment about the tin atom in spirocyclic amino alcohol derivatives of the latter.

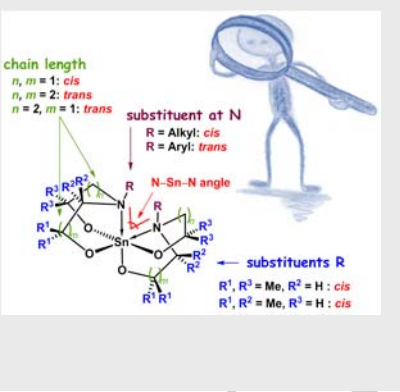

Britta Glowacki[a], Roman Pallach[a], Michael Lutter[a], Fabian Roesler[a], Hazem Alnasr[a], Cedreric Thomas[a], Dieter Schollmeyer[b], Klaus Jurkschat[a]*

Page No. – Page No.

***Cis* versus *Trans*: The Coordination Environment About the Tin(IV) Atom in Spirocyclic Amino Alcohol Derivatives**